The Probability of Quantal Secretion Near a Single Calcium Channel of an Active Zone

M. R. Bennett,* L. Farnell,† and W. G. Gibson†

*The Neurobiology Laboratory, Institute for Biomedical Research, Department of Physiology, and †The School of Mathematics and Statistics, University of Sydney, New South Wales 2006, Australia

ABSTRACT A Monte Carlo analysis has been made of calcium dynamics and quantal secretion at microdomains in which the calcium reaches very high concentrations over distances of <50 nm from a channel and for which calcium dynamics are dominated by diffusion. The kinetics of calcium ions in microdomains due to either the spontaneous or evoked opening of a calcium channel, both of which are stochastic events, are described in the presence of endogenous fixed and mobile buffers. Fluctuations in the number of calcium ions within 50 nm of a channel are considerable, with the standard deviation about half the mean. Within 10 nm of a channel these numbers of ions can give rise to calcium concentrations of the order of 100 μM. The temporal changes in free calcium and calcium bound to different affinity indicators in the volume of an entire varicosity or bouton following the opening of a single channel are also determined. A Monte Carlo analysis is also presented of how the dynamics of calcium ions at active zones, after the arrival of an action potential and the stochastic opening of a calcium channel, determine the probability of exocytosis from docked vesicles near the channel. The synaptic vesicles in active zones are found docked in a complex with their calcium-sensor associated proteins and a voltage-sensitive calcium channel, forming a secretory unit. The probability of quantal secretion from an isolated secretory unit has been determined for different distances of an open calcium channel from the calcium sensor within an individual unit: a threefold decrease in the probability of secretion of a quantum occurs with a doubling of the distance from 25 to 50 nm. The Monte Carlo analysis also shows that the probability of secretion of a quantum is most sensitive to the size of the single-channel current compared with its sensitivity to either the binding rates of the sites on the calcium-sensor protein or to the number of these sites that must bind a calcium ion to trigger exocytosis of a vesicle.

INTRODUCTION

The discovery of the synaptic vesicle associated proteins that are involved in exocytosis, such as the SNAP receptors synaptotagmin and synaptobrevin and the soluble *N*-ethyl maleimide-sensitive fusion protein attachment protein (SNAPs) syntaxin and SNAP 25, have greatly changed the conceptual framework within which quantal transmission can now be considered (Südhof, 1995). Indeed, synaptotagmin may well be the calcium sensor that triggers transmitter release on the arrival of an action potential (Brose et al., 1992). Of particular interest has been the discovery of a tight coupling between the voltage-dependent calcium channel that gates the entry of calcium for triggering exocytosis (whether N-type or P/Q-type) and a complex consisting of syntaxin and synaptotagmin (O'Connor et al., 1993; Yoshida et al., 1992; el Far et al., 1995; Martin-Moutot et al., 1996). The existence of a secretory unit of this kind has important implications for quantal transmission (Bennett, 1996). It is natural to associate a secretory unit with the concept of the "calcium microdomain," the region of high calcium concentration of the order of 100 μM that is calculated to occur within a distance ~25–50 nm from an open calcium channel (Simon and Llinás, 1985; Zucker and Fogelson, 1986). It has been suggested that these are the distances to be expected between the calcium channel and the calcium sensor among the vesicle associated proteins, probably synaptotagmin, although there is no direct evidence for these conjectures at this time (Yoshikami et al., 1989; Stanley, 1993).

There is evidence that secretory units significantly increase the efficiency of transmission at some synapses. Only one calcium channel need open in the avian ciliary ganglion terminal for a quantum of transmitter to be released, indicating that the calcium within a single microdomain is sufficient to trigger secretion (Stanley, 1993). Uncoupling the connection of domains II and III of the alpha I subunit of the N-type channel with syntaxin/SNAP 25 in the secretory unit leads to fragmentation of the units in motor nerve terminals, with a consequent 25% drop in evoked quantal release (Rettig et al., 1997). In addition, the observation that relatively slow calcium chelators such as ethylene glucol-bis(β-aminoethyl ether)-*N*,*N*,*N*′,*N*′-tetraacetic acid (EGTA) do not affect transmission at motor nerve terminals, whereas a fast chelator such as 1,2-bis(2-aminophenoxy)ethane-*N*,*N*,*N*,*N*-tetraacetic acid acetoxymethyl ester (BAPTA) does (Robataille et al., 1993), suggests that it is the high and relatively fast calcium transient in the microdomains that is responsible for triggering exocytosis in motor nerve terminals. Furthermore, the results of voltage clamp studies of transmitter release in the stellate ganglion of the squid indicate that single nonoverlapping calcium microdomains

Received for publication 6 November 1998 and in final form 8 February 2000.

Address reprint requests to Dr. M. R. Bennett, Neurobiology Laboratory F13, University of Sydney, NSW 2006, Australia. Tel.: 61-2-9351-2034; Fax: 61-2-9351-3910; E-mail: maxb@physiol.usyd.edu.au.

0006-3495/00/05/2201/21 $2.00

exist in the terminals, presumably within secretory units (Augustine et al., 1991). It would seem, then, that the calcium in microdomains of secretory units in both preganglionic and motor nerve terminals is dominant for triggering secretion. The importance attached to calcium in microdomains has prompted the present study.

A Monte Carlo description is given of the spatial distribution of calcium ions after they move out of an open channel and bind to the fixed and mobile buffers in region of domains after the opening of the channel. Calculations are given for channels having the properties of N-type calcium channels and opening spontaneously or under an action potential. These results are compared with the solutions of the transport equations that describe the buffered diffusion of calcium in the presence of rapid stationary and mobile calcium buffers (Wagner and Keizer, 1994). They are also compared with two approximations to the solutions, namely the rapid buffering approximation (Wagner and Keizer, 1994; Smith et al., 1996; Smith, 1996) and the linearized steady-state approximation (Neher, 1986; Pape et al., 1995; Naraghi and Neher, 1997). In addition, an analysis is given of the calcium changes in the volume of a varicosity or bouton in the presence of an indicator consequent on the opening of a single calcium channel, either spontaneously or under an action potential, and these results compared with those obtained from calculations that use deterministic equations to describe calcium movements in terminals (Sinha et al., 1997). Finally, the most appropriate set of parameters arrived at for the description of calcium dynamics in a microdomain is used in a Monte Carlo analysis of the probability of quantal release from vesicles. These are arranged in different spatial arrays about a channel and open either spontaneously or under an action potential.

A subsequent paper (Bennett et al., 2000) gives a Monte Carlo analysis of the probability of quantal release for the case where many secretory units are present at a nerve terminal and a number of their associated calcium channels open upon the arrival of a nerve impulse.

METHODS

In this section we outline the theory of calcium diffusion and buffering in a three-dimensional space, and then describe how this system can be simulated numerically using a Monte Carlo approach. The use of Monte Carlo methods in the context of transmitter release, diffusion, and binding was pioneered by Bartol et al. (1991) and subsequently applied in a number of related studies (Faber et al., 1992; Bennett et al., 1995b,c, 1996, 1997b, 1998). The following adapts the method to the case of calcium entering via a single channel, then diffusing and interacting with both fixed and mobile buffers, and binding to vesicle associated proteins. The region considered is a cubical box with 1-μm sides (Fig. 1). The plasmalemma is represented by the 1 μm $\times$ 1 μm base, lying in the *xy* plane, and calcium ions enter via a channel situated at the center of this plane. The other sides of the box represent the membrane walls of the terminal, and all six sides can contain calcium pumps that are incorporated into the Monte Carlo scheme as described below.

The Monte Carlo simulation method is an alternative to solving the reaction-diffusion equations, which are deterministic differential equations giving the temporal and spatial dependence of the average concentrations of the free calcium and of the various buffer complexes that may be present. A detailed comparison between the differential equation and the Monte Carlo approaches for the case of transmitter diffusion and binding has been given by Bartol et al. (1991) and many of the same arguments apply in the present case. In particular, the Monte Carlo approach is closer to the physical situation in that it gives some indication of the size of the stochastic fluctuations that are likely to occur. These can be very significant in the neighborhood of an open channel, where although the average calcium concentration can reach the order of 100 μM, this relatively high concentration is due to the presence of only a few calcium ions in a small volume. (In fact, for a concentration of 100 μM a cubic box with 100-nm sides would contain only $\sim$60 ions.)

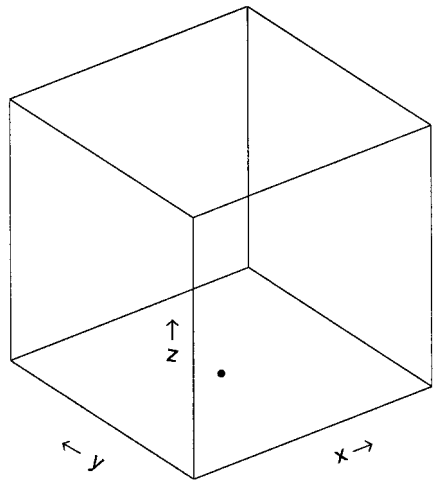

FIGURE 1 The Monte Carlo simulation uses a cubic box with 1-μm side length. The plasmalemma is represented by the 1 μm $\times$ 1 μm base; calcium ions enter via a channel situated in the center of the base. Calcium pumps are situated on all six walls of the box.

Calcium channels

Calcium channels in the plasmalemma can undergo either spontaneous or evoked opening. In the spontaneous case, a channel opens for a certain time T and during this time admits a constant current i_c; thus the input calcium current is a rectangular pulse. If the channel is assumed to have only two states, open and closed, then T is exponentially distributed (Bennett et al., 1995c, 1997a); that is, it has the density function

$$f_T(t) = \alpha e^{-\alpha t}, \quad t > 0 \tag{1}$$

where α is a constant. Thus T has mean and standard deviation equal to $1/\alpha$.

For the case of evoked release under an action potential, calcium channels open at different times for different durations, with therefore different driving forces on the calcium entry through the channels. A quantitative description of this has been given in the case of N-type calcium channels (Bennett et al., 1997a; see especially Fig. 4 in that paper). There, the way in which a single channel opens under a Hodgkin-Huxley action potential was investigated in detail with the opening and closing times, t_{open} and t_{close}, being modeled as nonhomogeneous Poisson processes with rate parameters that depend on the action potential, and hence are functions of time (compare Clay and DeFelice, 1983). The single-channel calcium current, $i_c(t)$, was also expressed as a function of the potential. The total charge q that enters through a single channel during the

course of an action potential can be found as

$$q = \int i_c(t)g(t)dt = \int_{t_{open}}^{t_{close}} i_c(t)dt, \quad (2)$$

where $g(t)$ is 1 if the channel is open and 0 otherwise; the second expression follows upon the assumption that a given channel opens at most once during the course of a single action potential. (Simulations showed that multiple openings were rare: Bennett et al., 1997a.)

Differential equations for calcium diffusion and buffering

The conventional way to characterize calcium diffusion and buffering is via differential equations that describe the spatial and temporal evolution of the various ionic and molecular species present. The buffering is assumed to be governed by the reaction

$$B_i + Ca^{2+} \underset{k_i^-}{\overset{k_i^+}{\rightleftharpoons}} CaB_i, \quad (3)$$

where Ca^{2+} represents free calcium ions, B_i represents unbound buffer molecules, and CaB_i represents calcium bound to buffer; $i = f$ for fixed buffer and $i = m$ for mobile buffer. The system is then governed by the equations (see, for example, Wagner and Keizer, 1994; Naraghi and Neher, 1997):

$$\frac{\partial[Ca^{2+}]}{\partial t} = D_{Ca}\nabla^2[Ca^{2+}] - k_f^+[Ca^{2+}][B_f] + k_f^-[CaB_f] - k_m^+[Ca^{2+}][B_m] + k_m^-[CaB_m] + \sigma(t)\delta(r), \quad (4)$$

$$\frac{\partial[B_m]}{\partial t} = D_{B_m}\nabla^2[B_m] - k_m^+[Ca^{2+}][B_m] + k_m^-[CaB_m], \quad (5)$$

$$\frac{\partial[CaB_m]}{\partial t} = D_{CaB_m}\nabla^2[CaB_m] + k_m^+[Ca^{2+}][B_m] - k_m^-[CaB_m], \quad (6)$$

$$\frac{\partial[B_f]}{\partial t} = -k_f^+[Ca^{2+}][B_f] + k_f^-[CaB_f], \quad (7)$$

$$\frac{\partial[CaB_f]}{\partial t} = k_f^+[Ca^{2+}][B_f] - k_f^-[CaB_f], \quad (8)$$

where $\sigma(t)$ is the calcium source density, assumed to be at the origin [$\delta(r)$ is a Dirac delta function] and D_α are the various diffusion coefficients. These equations can be solved directly, using suitable numerical techniques (see, for example, Smith et al., 1996). Also, a number of approximations have been developed. One of these, the rapid buffering approximation (Wagner and Keizer, 1994; Smith et al., 1996; Smith, 1996) utilizes the fact that the buffering kinetics act on a time scale that is much faster than the time scale for diffusion (see Appendix A), leading to the conclusion that the reaction described by Eq. 3 rapidly attains equilibrium, so that

$$[CaB_i] = \frac{[Ca^{2+}][B_i]_T}{K_i + [Ca^{2+}]}, \quad (9)$$

where $[B_i]_T = [B_i] + [CaB_i]$ is the total buffer concentration and $K_i = k_i^-/k_i^+$ is the dissociation constant for buffer i. Use of this approximation enables the set of Eqs. 4–8 to be replaced by a single differential equation describing the transport of calcium (Wagner and Keizer, 1994) and this has advantages for numerical solution (Smith et al., 1996) and for mathematical analysis (Smith, 1996).

A second approximation, valid for small calcium entry in the presence of a large concentration of mobile buffer, is the linearized steady-state approximation first given by Neher for the case where $[B_m]$ and $[CaB_m]$ are assumed constant (Neher, 1986) and later generalized to include the diffusion of B_m (Stern, 1992; Pape et al., 1995; Naraghi and Neher, 1997). This approximation gives the leading term in a perturbation expansion, the unperturbed state being the equilibrium state before calcium entry influx. It leads to the steady state calcium concentration being given by (Pape et al., 1995; Naraghi and Neher, 1997)

$$[Ca^{2+}] = c_0 + \frac{\sigma}{2\pi D_c}\frac{1}{r}e^{-r/\lambda} + \frac{\sigma}{2\pi D_c}\frac{\lambda^2}{\lambda_m^2}\frac{1}{r}(1 - e^{-r/\lambda}), \quad (10)$$

where $c_0 \equiv [Ca^{2+}]_0$ is the background calcium level, σ is the constant source density, assumed to be into a hemisphere, λ is a space constant given by $1/\lambda^2 = 1/\lambda_c^2 + 1/\lambda_m^2$ where $\lambda_c = \sqrt{D_c/k_m^+[B_m]_0}$ is the characteristic length for binding of diffusing calcium, and $\lambda_m = \sqrt{D_m/(k_m^+c_0 + k_-)}$ is the corresponding quantity for the mobile buffer ($D_c \equiv D_{Ca}$, $D_m \equiv D_{B_m}$). If $\lambda_c \ll \lambda_m$, the last term in Eq. 10 can be neglected and λ can be replaced by λ_c in the second term, which recovers the earlier expression of Neher (1986).

Monte Carlo method

The following sections give details of the Monte Carlo simulation scheme. This is implemented via a computer program written in Fortran and run on a Digital Alpha workstation. The pseudo-code used is given in Appendix B.

Diffusion of calcium

In the Monte Carlo method, the motion of each individual calcium ion is followed as it diffuses inside the terminal. The motion is not followed at the level of the actual Brownian motion but at a coarser level, using a timestep Δt (of the order of 1 μs) during which the ion is assumed to move in a straight line. The distance travelled is a random variable that depends on Δt and on the diffusion coefficient $D_c \equiv D_{Ca}$.

The equation for unrestricted diffusion in three-dimensional space is

$$\frac{\partial c}{\partial t} = D_c\nabla^2 c = D_c\left(\frac{\partial^2 c}{\partial x^2} + \frac{\partial^2 c}{\partial y^2} + \frac{\partial^2 c}{\partial z^2}\right), \quad (11)$$

where $c \equiv c(x, y, z, t)$ is the density of the diffusing particles at point (x, y, z) at time t. From this, it follows that if a particle starts from the origin at time $t = 0$ and reaches the point (X, Y, Z) at time t, then each Cartesian coordinate X, Y, Z is an identically distributed Gaussian random variable with density function

$$f_W(w, t) = \frac{1}{\sqrt{4\pi D_c t}}e^{-w^2/4D_c t}, \quad (12)$$

where $W = X$, Y or Z and $w = x$, y, or z, respectively. The average distance travelled parallel to any coordinate axis in time t is $E(|W|) = 2\sqrt{D_c t/\pi}$, so in time Δt the average increment in any coordinate is

$$\bar{L} = \sqrt{4D_c\Delta t/\pi}. \quad (13)$$

The actual increment $L = |W|$ in each coordinate can be found by generating random numbers using the distribution in Eq. 12. It is convenient to relate this to the random variable U, uniformly distributed on (0, 1), by $L = \sqrt{4D_c\Delta t}\ \mathrm{erf}^{-1}(U)$, where erf^{-1} is the inverse error function. A practical formula, based on dividing the distribution into 100 bins of equal proba-

bility, is (Bartol et al., 1991)

$$L = \sqrt{4D_c\Delta t}\,\mathrm{erf}^{-1}((j - 0.5)/100), \tag{14}$$

where j takes integer values uniformly distributed on [1, 100]. This method has been used in the calculations presented here. For species other than free calcium, D_c is to be replaced by the appropriate diffusion coefficient in the above formulas.

For the single calcium channel considered here, calcium entry is assumed to take place at the origin into the half-space $z > 0$; the number of Ca^{2+} entering during each timestep Δt can be calculated from the single-channel current i_c using the fact that a calcium current of 1 pA corresponds to ~3120 Ca^{2+}/ms. In each time interval Δt the x, y, and z coordinates of each calcium ion in the system are updated by adding $\pm L$ to each coordinate where + or − is chosen at random (with equal probability), and the values for L are generated as described above. That is, in the time interval Δt the ion moves, in a straight line, from position (x, y, z) to position $(x + \Delta x, y + \Delta y, z + \Delta z)$, where the increments Δx, Δy, and Δz are chosen from the distribution with density function (Eq. 12). The major part of the calculation is now bookkeeping: at the end of each timestep the current coordinates of each calcium ion are recorded and then used as the initial conditions for the next step. The simplest case is when the ion remains inside the terminal during the timestep so the new coordinates can be immediately recorded. If the ion's displacement during Δt is such that it would cross a wall of the terminal, then it is assumed to undergo specular reflection; that is, the motion parallel to the wall is unchanged but the component perpendicular to the wall is reversed. Other possibilities concern the interaction with buffers and indicators, the effect of ionic pumps in the terminal walls, and the binding of calcium ions to vesicle-associated proteins at the plasmalemma. The incorporation of each of these effects into the Monte Carlo scheme is described below.

It should be mentioned that although background calcium of concentration $c_0 = [Ca^{2+}]_0$ is present throughout the system, it is not explicitly included in the Monte Carlo calculation, which involves only excess calcium. Thus, the calculations involve $[Ca^{2+}]_{excess}$ given by

$$[Ca^{2+}]_{excess} = [Ca^{2+}]_{actual} - c_0 \tag{15}$$

where $[Ca^{2+}]_{actual}$ is the actual concentration. Allowance for this use of excess calcium is made when required, as described in the sections below.

Fixed buffer

The fixed buffer is taken to be distributed uniformly with density $[B_f]_T$ throughout the volume under consideration. The calcium ions bind reversibly to the buffer molecules according to Eq. 3 with $i = f$. Some of the initial fixed buffer molecules bind to the background calcium present in the terminal; using the steady-state form of Eq. 7 with $[Ca^{2+}] = c_0$ and $[B_f] = [B_f]_{excess}$, where $[B_f]_{excess}$ is the residual fixed buffer concentration, gives $-k_f^+ c_0[B_f]_{excess} + k_f^-[CaB_f] = 0$. But $[B_f]_{excess} = [B_f]_T - [CaB_f]$, leading to

$$[B_f]_{excess} = \frac{K_f[B_f]_T}{K_f + c_0}, \tag{16}$$

where $K_f = k_f^-/k_f^+$. (For the values of K_f and c_0 given in Table 1 below, $[B_f]_{excess}$ is ~99% of $[B_f]_T$.) In order to incorporate the fixed buffer into the Monte Carlo scheme, we first divide the total volume into equal cubes of volume ΔV such that each cube contains one buffer molecule and the overall density is $[B_f]_T = 1/\Delta V$. A number of these molecules, chosen at random, are assumed to be bound to background calcium so that the remaining unbound buffer molecules have density $[B_f]_{excess}$, as given by Eq. 16. The background bound buffer molecules are assumed to remain bound and so effectively no longer enter into the computation; in addition, as discussed above under calcium diffusion, only excess calcium ions are considered in the Monte Carlo simulation. It is estimated that the total error introduced by this joint approximation is <1% for the parameters used in the calculations reported here (see Appendix A). At each timestep Δt suppose that a calcium ion in a cube containing an unbound buffer molecule binds to that molecule with probability p_+. Then the average number of bindings in time Δt in that cube will be $[Ca^{2+}]_{excess}\Delta V p_+$; but from Eq. 3 this average is also given by $k_f^+[Ca^{2+}]_{excess}\Delta t$, leading to an expression for the binding probability p_+ in terms of the forward binding rate k_f^+:

$$p_+ = k_f^+[B_f]_T\Delta t. \tag{17}$$

It is assumed that unbinding is a Poisson process with rate constant k_f^-, so the bound buffer molecules unbind in timestep Δt with probability p_- given by Bartol et al., 1991

$$p_- = 1 - \exp(-k_f^-\Delta t) \approx k_f^-\Delta t. \tag{18}$$

(For the parameter values given in Table 1, $p_+ \approx 0.11$ and $p_- \approx 0.004$.)

Mobile buffer

The mobile buffer is taken to be initially distributed uniformly throughout the volume under consideration with density $[B_m]_T$. The calcium ions bind reversibly to the buffer molecules according to Eq. 3 with $i = m$. The principal difference to the fixed buffer case is that now, as well as the calcium ions diffusing, both the buffer molecules B_m and the bound molecules CaB_m diffuse. Theoretically, the Monte Carlo scheme could be modified to keep track of all these species, but this would both slow the calculation and the additional bookkeeping needed would limit the size of system that could be simulated. Therefore, an approximate scheme has been implemented based on dividing the space into equal cubic cells that each contain the same number of mobile buffer molecules. Again, an adjustment must be made for binding to the background calcium, and this reduces the initial density from $[B_m]_T$ to $[B_m]_{excess}$ given by (cf. Eq. 16)

$$[B_m]_{excess} = \frac{K_D[B_m]_T}{K_D + c_0}. \tag{19}$$

(See Appendix A for a discussion of the accuracy of this approximation.) It is now assumed that binding probabilities are uniform over each cubic cell and proportional to the number of unbound mobile buffer molecules in that cell. A crucial further assumption is that both unbound (B_m) and bound (CaB_m) molecules diffuse at the same rate, so that the total buffer concentration ($[B_m] + [CaB_m]$) remains uniform throughout the whole volume, and hence the average number of unbound plus bound buffer molecules in each cell remains constant. (The assumption that both the free and the complexed form of a buffer species have the same diffusion coefficient is also made by Klingauf and Neher, 1997.) If fluctuations about this average are neglected, then it is sufficient to track the bound molecules (CaB_m), updating their positions at each timestep using increments from the distribution (Eq. 12), but with D_c replaced by D_{B_m}. Each time the count of CaB_m molecules within a cell changes (by binding, unbinding, or diffusion of CaB_m from one cell to another) the population of that cell is recomputed, so that ($[B_m] + [CaB_m]$) remains constant. In this way, it is not necessary to explicitly follow the diffusion of the unbound buffer molecules B_m. The binding probabilities are immediately adjusted when the cell population changes, and this may occur several times in the same timestep. For a given cell, this probability is (compare Eq. 17)

$$p_+ = \lambda k_m^+[B_m]_{excess}\Delta t, \tag{20}$$

where λ is the ratio of unbound to total mobile buffer molecules in that cell. The unbinding probability is again given by Eq. 18. This method of handling the mobile buffer involves little more bookkeeping than was required for the calcium alone, the main addition being a table of cell populations. (The good agreement obtained between the Monte Carlo

TABLE 1 Values of the parameters used in the numerical calculations

Quantity	Symbol	Value	Cell Type	Notes
Calcium				
Diffusion coefficient	D_{Ca}	220 $\mu m^2\ s^{-1}$	Neuroendocrine	Klingauf and Neher (1997)
Background concentration	c_0	0.1 μM		
Fixed buffer				
Total concentration	$[B_f]_T$	300 μM	〃	〃
Dissociation constant	K_f	10 μM	〃	〃
Forward binding rate	k_f^+	$5 \times 10^8\ M^{-1}\ s^{-1}$	〃	〃
Mobile buffer				
Total concentration	$[B_m]_T$	100 μM	〃	〃
Dissociation constant	K_m	10 μM	〃	〃
Forward binding rate	k_m^+	$5 \times 10^8\ M^{-1}\ s^{-1}$	〃	〃
Diffusion coefficient	D_{B_m}	15 $\mu m^2\ s^{-1}$	〃	〃
Exogeneous buffers: Fura-2				
Total concentration	$[B_i]_T$	100 μM	〃	〃
Dissociation constant	K_i	0.24 μM	〃	〃
Forward binding rate	k_i^+	$5 \times 10^8\ M^{-1}\ s^{-1}$	〃	〃
Diffusion coefficient	D_{B_i}	50 $\mu m^2\ s^{-1}$	〃	〃
Exogeneous buffers: Furaptra				
Total concentration	$[B_i]_T$	100 μM		As for fura-2
Dissociation constant	K_i	60 μM	Hippocampal	Sinha et al. (1997)
Forward binding rate	k_i^+	$5 \times 10^8\ M^{-1}\ s^{-1}$		As for fura-2
Diffusion coefficient	D_{B_i}	50 $\mu m^2\ s^{-1}$		〃
Calcium pumps				
Pump density	σ_P	2000 μm^{-2}	Hair cell stereocilia	Yamoah et al. (1998)
Maximum pumping rate	V_P	3.2×10^{-11} mol $cm^{-2}\ s^{-1}$		see Discussion
Dissociation constant	K_P	0.2 μM	Smooth muscle	Kargacin and Fay (1991)
Vesicle binding ("Standard")				
Attachment rate	k^a	$15 \times 10^6\ M^{-1}\ s^{-1}$	Chromaffin, bipolar	Bennett et al. (1997a)
Detachment rate	k^d	750 s^{-1}	Range of cell types	〃
Conformational change rate	β	2000 s^{-1}	Range of cell types	〃
Monte Carlo				
Timestep	Δt	0.75 μs		
Vesicle disc radius	r_V	10 nm		

calculations and calculations based on the differential equation approach, see Fig. 5 below, indicates that this approximation is justified.)

This approximate treatment of the mobile buffer does lead to some small inaccuracies, particularly in $[CaB_m]$. If the cubic cells are made too large, then the assumption of uniform binding probabilities in each cell is not valid; however, making the cells too small encounters the problem that each cell must contain an integral number of molecules. Thus a compromise must be found; in the calculations reported here, the cubes have sides of ~50 nm and each contains about seven buffer molecules. Calculations are also performed using the indicators fura-2 and furaptra; these are treated in the same way as the mobile buffer, using the appropriate diffusion and binding rates (see Table 1).

Calcium pumps

At the plasmalemma and at any other terminal boundary the diffusing molecules are mirror-reflected as described above (unless they bind to vesicles or pumps, as described below). In a number of calculations, a cubic box with 1-μm sides is used to represent the terminal, and all its sides are reflecting walls. In other calculations, where only effects near the plasmalemma are being considered, the volume considered is a cube with 1-μm sides, but only the side representing the plasmalemma is a reflecting wall; the other sides are transparent, and once a molecule passes through them it is lost and no longer included in the bookkeeping.

Calcium pumps occur both in the plasmalemma and in the other walls of the terminal. The pumping is represented as a "tunneling" process in which the cytoplasmic calcium ion first binds (irreversibly) to the pump, and then upon unbinding is ejected from the terminal:

$$(Ca)_{cyt} + P \overset{k_1}{\rightarrow} CaP \overset{k_2}{\rightarrow} (Ca)_{ext} + P. \tag{21}$$

This process must now be incorporated into the Monte Carlo scheme. Following Bartol et al.'s treatment of receptor and of esterase binding, it is assumed that the membrane walls are "tiled" with squares of side length $1/\sqrt{\sigma_P}$, where σ_P is the pump density and that each square contains one pump. To bind to an available pump a calcium ion must first hit the square containing that pump; this will be determined by the line joining its position at the beginning and at the end of the interval Δt. Assuming that it hits, it will then bind with a probability p_+, which is related to the corresponding binding rate k_1 by (cf. Bartol et al., 1991, Eq. 6a)

$$p_+ = k_1 \sigma_P \sqrt{\frac{\pi \Delta t}{D_c}}. \tag{22}$$

If the ion fails to bind, or if it hits a square where the pump molecule is already bound, then it undergoes specular reflection, as described above. The unbinding probability per timestep does not depend on the calcium diffusion and is simply given by

$$p_- = 1 - \exp(-k_2 \Delta t) \approx k_2 \Delta t. \tag{23}$$

The rate coefficients k_1 and k_2 are not directly measurable. To get estimates it is necessary to relate them to the usual parameters describing lumped calcium extrusion through a plasma membrane. The standard expression for the flux due to pumping is $-V_P[Ca^{2+}]_{actual}/(K_P + [Ca^{2+}]_{actual})$, where V_P and K_P are constants (Sala and Hernandez-Cruz, 1990; Kargacin and Fay, 1991; Nowycky and Pinter, 1993). If we assume that there is also a constant inward leak that just balances the pump at the resting calcium level c_0, then $[Ca^{2+}]_{excess}$ satisfies

$$\frac{d[Ca^{2+}]_{excess}}{dt} = -\frac{\hat{V}_P[Ca^{2+}]_{excess}}{[Ca^{2+}]_{excess} + \hat{K}_P}, \tag{24}$$

where $\hat{V}_P = V_P K_P/(K_P + c_0)$ and $\hat{K}_P = K_P + c_0$. This can be related to the Monte Carlo scheme by applying the Michaelis-Menten approximation to Eq. 21 (e.g., Murray, 1993), leading to the following expression for the rate of calcium extrusion:

$$\frac{d[Ca^{2+}]_{excess}}{dt} = -\frac{k_2\sigma_P[Ca^{2+}]_{excess}}{[Ca^{2+}]_{excess} + k_2/k_1}, \tag{25}$$

where $[Ca^{2+}]_{excess}$ is the excess calcium concentration inside the terminal, defined by Eq. 15. Comparing Eq. 25 with Eq. 24 gives $k_2 = \hat{V}_P/\sigma_P$ and $k_1 = k_2/\hat{K}_P$. Note that in the above way of assigning parameter values the pump density, σ_P, is, within reasonable limits, an arbitrary parameter. Once σ_P has been given a value, k_1 and k_2 are then chosen to give the desired pumping rate.

Vesicles and exocytosis

The standard assumption will be that calcium ions bind to the vesicle-associated proteins according to the scheme (Heidelberger et al., 1994; Heinemann et al., 1994)

$$S_0 \underset{\nu_1}{\overset{4\mu_1}{\rightleftharpoons}} S_1 \underset{2\nu_2}{\overset{3\mu_2}{\rightleftharpoons}} S_2 \underset{3\nu_3}{\overset{2\mu_3}{\rightleftharpoons}} S_3 \underset{4\nu_4}{\overset{\mu_4}{\rightleftharpoons}} S_4 \overset{\beta}{\rightarrow} S_{ex}, \tag{26}$$

where S_i, $i = 1, \ldots, 4$ denotes the state with i sites occupied, S_{ex} denotes the state with four sites occupied after the conformational change, $\mu_i(t)$ ($\nu_i(t)$) are the rates of attachment (detachment) of a calcium ion at the ith step, and $\beta(t)$ is the rate for the final step. These attachment rates μ_i are taken to be proportional to the excess calcium concentration at the position of the vesicle-associated protein, and the detachment rates ν_i are taken to be constants, independent of time:

$$\mu_i = k_i^a c(r, t); \quad \nu_i = k_i^d; \quad i = 1, \ldots, 4, \tag{27}$$

and the conformational change rate β is taken to be a time-independent constant. A further simplification is to assume no cooperativity in binding or unbinding, in which case $k_i^a = k^a$ and $k_i^d = k^d$, $i = 1, \ldots, 4$. The above single-affinity scheme for the binding of calcium to the vesicle-associated proteins has been used to describe calcium-dependent exocytosis at synapses formed by goldfish retinal bipolar cells (Heidelberger et al., 1994) and bovine chromaffin cells (Heinemann et al., 1994). A more complex scheme may be used in which the binding sites have different affinities, although an investigation of such kinetics indicates that the results obtained for the probability of secretion are not much different from those for the single-affinity case (see Fig. 7 in Bennett et al., 1997a).

To incorporate this into the Monte Carlo scheme, we again follow Bartol et al.'s treatment of receptor binding and assume that the plasmalemma is "tiled" with squares whose size is determined by the geometric placement and the density of the vesicle array being modeled. The vesicle binding site is represented as a disk of radius r_V placed at the center of selected tiles. To bind, a calcium ion must first hit the disk [which will be determined by whether its free path during the interval Δt would pass through the tile, this path being the straight line from point (x, y, z) to point $(x + \Delta x, y + \Delta y, z + \Delta z)$]; it will then bind with probability p_+, which is related to the corresponding forward binding rate k_+ by (compare Eq. 22):

$$p_+ = \frac{k_+}{a_V}\sqrt{\frac{\pi\Delta t}{D_c}}, \tag{28}$$

where $a_V = \pi r_V^2$ is the area of the vesicle disk. If it does not bind it is reflected in the usual way. The binding probabilities change according to how many calcium ions are already bound; for the binding of the ith calcium ion, where $i = 1, \ldots, 4$, p_+ is given by Eq. 28 with $k_+ = (5 - i)k^a$.

The unbinding per timestep does not depend on the calcium concentration and is given by (cf. Eq. 18)

$$p_- = 1 - e^{-k_-\Delta t} \approx k_-\Delta t, \tag{29}$$

where $k_- = ik^d$, $i = 1, \ldots, 4$ is the relevant rate constant. The conformation change is treated using a similar formula.

Other schemes have also been proposed with different Ca^{2+} stoichiometries, requiring the binding of either three or two Ca^{2+} before the final conformational change leading to exocytosis (Heinemann et al., 1993; 1994). These will be used as a comparison with the four-binding case given by Eq. 26.

Parameter choice

The main parameter values used in the calculations are listed in Table 1. Some comments on these choices can be found in the Discussion section.

RESULTS

The Monte Carlo results are divided into two main sections. The first of these is concerned with establishing the calcium transients that occur immediately about a single open N-type calcium channel; in addition, the transients of free calcium and of indicator calcium in the volume of a varicosity or bouton are considered. The second section is concerned with using the information provided by the previous section to establish how a calcium transient at a secretory unit triggers vesicle exocytosis following an action potential, when these vesicles are arranged in different configurations with respect to the channel.

In all cases the terminal contains a mobile buffer with the characteristics of calmodulin and a fixed buffer with the characteristics of calbindin (see Table 1). In addition, a calcium indicator is sometimes present, which is either furaptra, representative of a low-affinity indicator, or fura-2, representative of a high-affinity indicator. Unless otherwise mentioned, all values of free calcium and of calcium bound to the various buffers are the means of at least five trials, where each trial is a Monte Carlo simulation using the same parameters and initial conditions, but different random numbers. If standard deviations are also given, then at least 10 trials were used. (The expression $\sqrt{\Sigma_i(X_i - \bar{X})/n}$ is used for the standard deviation; the alternative expression involving $n - 1$ in place of n will give values differing by at most 5%, and this difference would be undetectable on the graphs.)

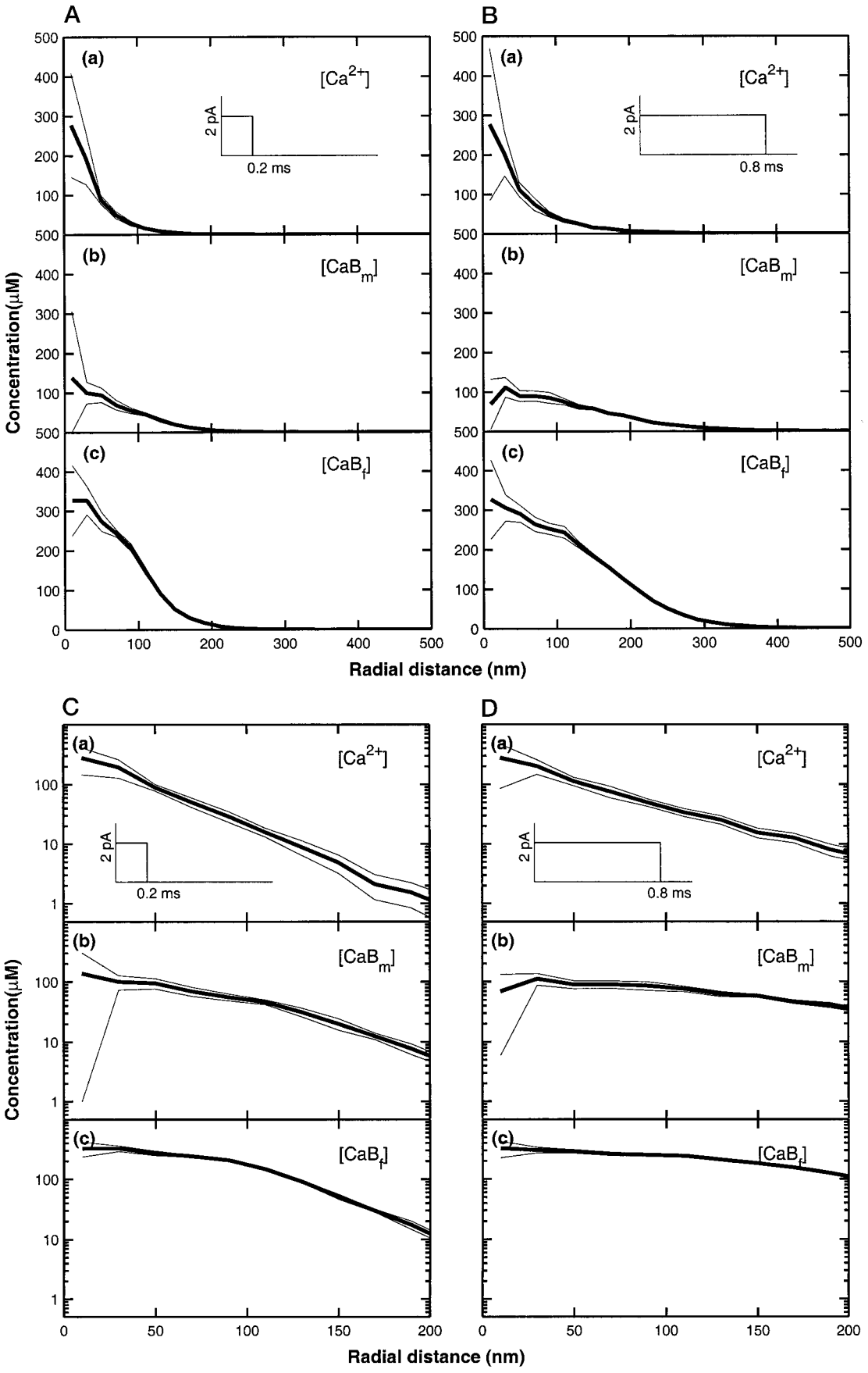
A
B
C
D
(a)
(b)
(c)
[Ca2+]
[CaBm]
[CaBf]
2 pA
0.2 ms
0.8 ms
Concentration(μM)
Radial distance (nm)

Calcium microdomains

Spontaneous opening

The properties of N-type calcium channels indicate that at the resting potential the average open time of a channel is 0.2 ms and passes a current of ~2 pA (Bennett et al., 1997a). However, it is the longer and much less frequent open times of ~0.8 ms that are likely to have a major effect on triggering exocytosis. Monte Carlo simulations have been performed to obtain the concentration profile of calcium about a single spontaneously opening N-type calcium channel with each of these sets of characteristics. The Monte Carlo scheme gives the coordinates of each calcium ion, free or bound, at each time step, and these can be converted to concentrations using appropriate binning. To show the change of concentration with distance from the release site the bins were chosen to be hemispherical shells of radius r and thickness Δr ($=20$ μm); at a given time the numbers of each species of particle in a shell (r, $r + \Delta r$) are counted and then converted to a number density by dividing by the shell volume $2\pi r\Delta r$, and finally to a concentration using the fact that 1 μM corresponds to ~600 molecules per μm^3. The results are shown in Fig. 2, *A* and *B* in normal coordinates and in Fig. 2, *C* and *D* using logarithmic ordinates. At the end of the 0.2-ms open time of the channel there is a high concentration of calcium bound to the fixed buffer in the immediate vicinity of the channel, about 327 μM, which decays approximately biexponentially with length constants of ~144 nm over the first 100 nm and then 33 nm over the next 200 nm (Fig. 2, *Ac* and *Cc*). In contrast, there is a much smaller amount of calcium bound to the mobile buffer near the channel, ~100 μM, which also decays away biexponentially with length constants of ~88 nm and then 38 nm (Fig. 2, *Ab* and *Cb*). These effects of the fixed and free buffer ensure a relatively steep gradient of free calcium near the channel that falls off from a concentration of 277 μM within 10 nm of the channel with a length constant of ~33 nm (Fig. 2, *Aa* and *Ca*). Similar results are found for the case in which the channel opens for longer times, such as 0.8 ms (Fig. 2, *B* and *D*). The main difference is that the buffers retain more calcium for greater distances from the channel than in the shorter opening time case (compare Fig. 2 *Ab* with 2 *Bb* and 2 *Ac* with 2 *Bc*). Even so, the slope of the free calcium at 30 nm from the channel remains steeper for the former case (compare Fig. 2 *Aa* with 2 *Ba*). However, the free calcium concentration within 10–20 nm of the channel is about the same at the end of the shorter opening time and the longer opening time, because in the latter case there has been sufficient time for the endogenous buffers to exert considerable effect on the free calcium at this distance. The standard deviations in the extent of free calcium ~30 nm from the channels are very large, and amount to about half the mean (Fig. 2, *Aa* and *Ba*). Thus, even for a nonstochastically opening channel, there will be large fluctuations in the calcium concentration at distances from the channel mouth at which calcium-sensor proteins for exocytosis are expected to be found.

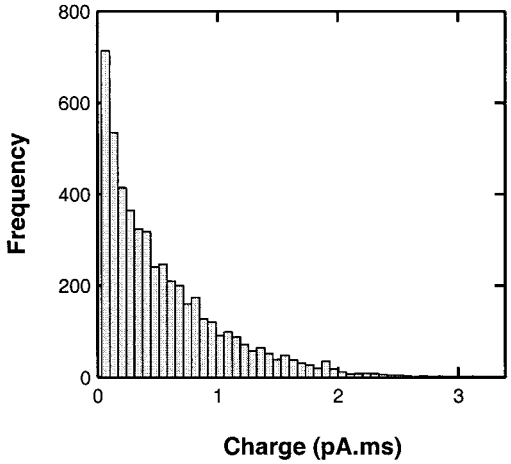

FIGURE 3 Frequency distribution of the total calcium charge that passes through a single N-type channel when it opens under an action potential. The total charge that enters during a single action potential is found using Eq. 2, where the opening and closing times, t_{open} and t_{close}, and the single-channel current, $i_c(t)$, are calculated as in Bennett et al. (1997a). The histogram shows the frequency of occasions during five thousand action potentials at which a particular charge (pA · ms) is passed by the channel. (1 pA · ms = 10^{-15} Coulombs and corresponds to the charge on 3120 calcium ions.) The histogram is well-fitted by an exponential distribution with mean 0.52 and standard deviation 0.50 pA · ms.

Evoked opening

For the case of evoked opening the total charge that enters through a single channel is given by Eq. 2. A histogram

FIGURE 2 The mean and standard deviation of the spatial calcium concentration profile near a single spontaneously opening channel at the end of the open time of the channel. The channel opens deterministically and admits a constant current. The calculations are performed using the Monte Carlo scheme, which gives the position of each calcium ion at each time step; these positions are converted to densities using hemispherical bins of 20-nm thickness. (*A*) Results for the average open time of an N-type channel of 0.2 ms (see Fig. 5 *A* in Bennett et al., 1995a) with a current of 2 pA; the time course of this current is shown as an inset in *Aa*. (*B*) Results for a relatively long open time of 0.8 ms and current of 2 pA; the time course is shown as an inset in *Ba*. In each case, panels *a–c* give the concentrations of free calcium ($[Ca^{2+}]$), of calcium bound to the mobile buffer ($[CaB_m]$), and the calcium bound to the fixed buffer ($[CaB_f]$), respectively. (*C*) and (*D*) show the corresponding results using log ordinates. The parameters used in the calculations are given in Table 1. In each graph, the heavy line shows the mean concentration (in μM) and the thin lines show one standard deviation away from the mean; these are the result of 10 Monte Carlo simulations, each run starting from the same initial conditions with the same calcium influx (but using different random numbers).

showing the results of 5000 simulations of a single channel under a Hodgkin-Huxley action potential is given in Fig. 3. The charge turns out to be approximately exponentially distributed; as calculated from the simulation results, it has mean 0.52 pA · ms ($=0.52 \times 10^{-15}$ Coulombs) and standard deviation 0.50 pA · ms. (That the charge should be exponentially distributed is not obvious. For the spontaneous case, the charge through a single channel is indeed exponentially distributed, but this is a direct consequence of the exponentially distributed channel open time and the constant current through it: see Fig. 5 *A* in Bennett et al., 1995a. For the evoked case, there is a complicated interplay between open time, which is not exponentially distributed, and nonconstant single channel current.) The mean open duration for an N-type calcium channel under an action potential is 0.84 ms (see Fig. 4 *B* in Bennett et al., 1997a); given that the average charge is 0.52 pA · ms, then the average current is 0.62 pA. However, as in the spontaneous case, it is the longer and less frequent open times that are likely to be important in triggering exocytosis, so consideration has also been given to an open time of 1.0 ms and a charge of 1.5 pA · ms, giving an average current of 1.5 pA.

The free calcium about a channel opening under an action potential with these two sets of characteristics (namely 0.62 pA for 0.84 ms and 1.5 pA for 1.0 ms) have therefore been computed using Monte Carlo simulation. Fig. 4 shows that the longer duration opening channel has much greater free calcium within 30 nm of the channel (Fig. 4 *Ba*) than does the shorter duration opening channel (Fig. 4 *Aa*), because the former passes 4680 calcium ions and the latter only 1625 ions. As in the spontaneous case, the standard deviations in the amount of free calcium near the channels are at least half of the mean (Fig. 4, *Aa* and *Ba*), indicating that considerable fluctuations in quantal release from impulse to impulse may be expected on the basis of the fluctuations in the amount of calcium that reaches the calcium sensor proteins for exocytosis.

Rapid buffering and linearized diffusion approximation

Fig. 5 shows the levels of free calcium and of calcium bound to the fixed and mobile buffers as functions of distance from a channel that passes 2 pA of current and opens for 0.8 ms; the profiles are shown at the end of the

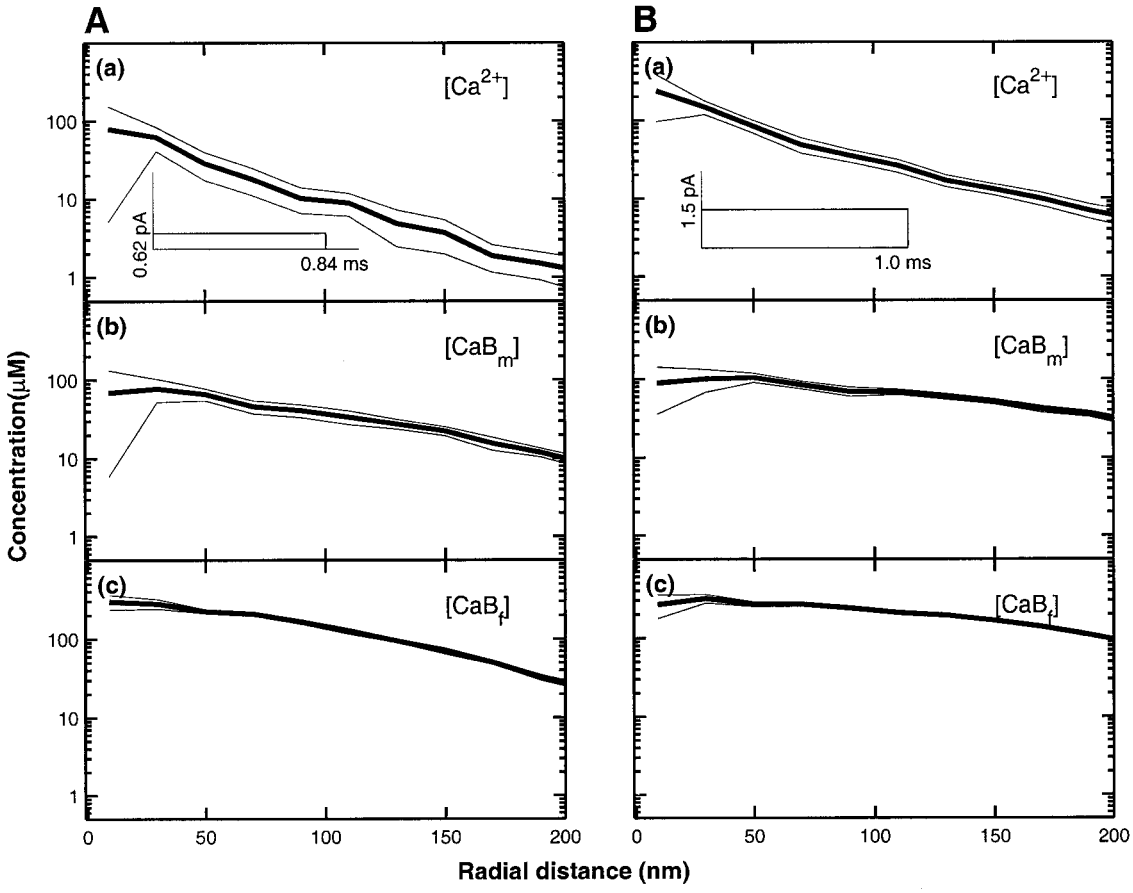

FIGURE 4 As for Fig. 2, except that the single channel now opens under an action potential. (*A*) Results for the average open time of an N-type channel of 0.84 ms (see Fig. 4 *B* in Bennett et al., 1997a) with a current of 0.62 pA. (*B*) Results for a relatively long open time of 1.0 ms and current of 1.5 pA according to the mean charge in Fig. 3.

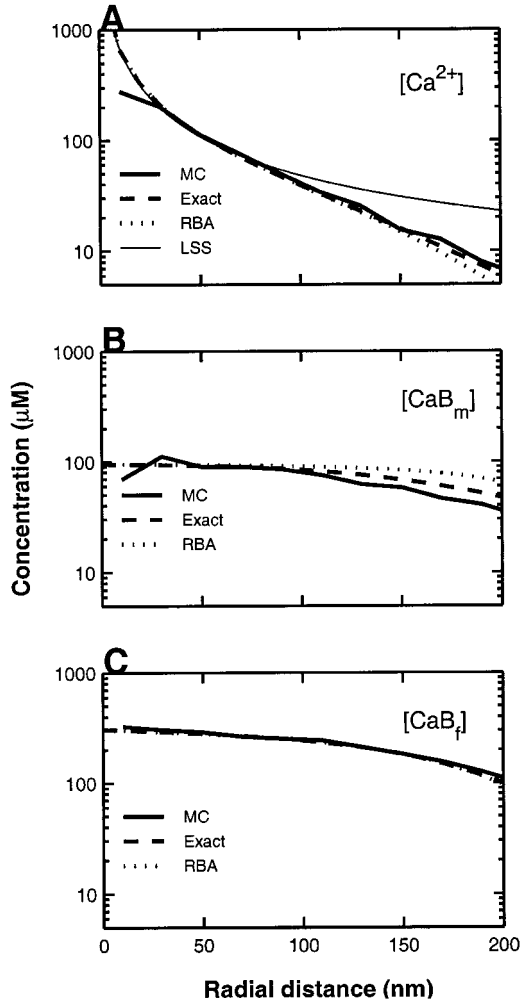

FIGURE 5 Comparison between the Monte Carlo (MC) calculation of the calcium profile near a single channel opening spontaneously (*continuous heavy lines*) and the results using the deterministic differential Eqs. 4–8 (*dashed lines*). Also shown are the results obtained using the rapid buffering approximation (RBA) given by Eq. 9 (*dotted lines*), and in *A* the thin continuous line is calculated using the linearized steady-state approximation (LSS) given by Eq. 10. Calculations are for the long open time of an N-type channel of 0.8 ms with a current of 2 pA. *A–C* give the concentrations of free calcium ($[Ca^{2+}]$), of calcium bound to the mobile buffer ($[CaB_m]$), and of calcium bound to the fixed buffer ($[CaB_f]$), respectively. The parameters used in the calculations are given in Table 1. Log ordinates.

opening period. The heavy solid lines are the averages of 10 Monte Carlo simulations. (Compare Fig. 2 *B*, which shows the same results together with standard deviations.) The broken lines come from solving the deterministic differential Eqs. 4–8, which in this case reduce to one spatial dimension because spherical symmetry allows the Laplacian operator to be simplified to $\nabla^2 = \partial^2/\partial r^2 + (2/r)\partial/\partial r$, where r is the radial coordinate. The method used is basically that given in the Appendix of Smith et al. (1996), except that a fourth-order Runge-Kutta routine is used for the time (Press et al., 1989). Agreement is excellent except for short distances, where the Monte Carlo simulations indicate that large fluctuations occur (see Fig. 2 *B* for standard deviations). There is also some discrepancy in $[CaB_m]$ at distances >100 nm (Fig. 5 *B*); this can be traced to an inherent limitation in the approximation made in treating the mobile buffer in the Monte Carlo simulation (see the Methods section for a discussion of this).

Also shown (*dotted lines*) are the results obtained using the rapid buffering approximation (Eq. 9) (Wagner and Keizer, 1994; Smith et al., 1996). Because in the present case the buffer kinetics are fast compared to the diffusion, it is expected that this approximation will be good (see Appendix A), and this is indeed borne out by the results (Fig. 5). Somewhat surprising, however, is that the linearized steady-state approximation (Pape et al., 1995; Naraghi and Neher, 1997), as given by Eq. 10, gives an accurate representation of the free calcium profile at distances $<\sim$100 nm (Fig. 5 *A*, *thin continuous line*); this approximation is derived under the condition that the mobile buffer is far from saturation, which is not the case here. (See Fig. 5 *B*; the total mobile buffer concentration is only 100 μM.)

Ca^{2+} transients of a varicosity or bouton

The question arises as to whether it is possible to detect the changes in calcium concentration in the entire volume of a varicosity or bouton when a calcium channel opens either spontaneously or under an action potential. Monte Carlo calculations have been made of calcium transients for the average open times of both the spontaneous and evoked opening of a calcium channel. The channel is placed in the center of one of the six walls of a cubic volume with 1-μm side (Fig. 1), these being the approximate dimensions of small varicosities and boutons. In this case it is important to allow for the action of calcium pumps, as the only way that calcium ions can be removed from this volume, after being released from the endogenous buffers, is through such a mechanism. To this end we have modeled such pumps so that they may be included in the Monte Carlo simulations and distributed them over all six walls of the cubic volume (see Methods). Fig. 6 *A* shows the results for the spontaneous opening (0.2 ms and 2 pA), and Fig. 6 *B* those for the evoked opening (0.84 ms and 0.62 pA), for the case where no indicator is present. In each case, *curve a* gives the mean and standard deviation of the free calcium, *b* gives the calcium bound to the fixed buffer, and *c* gives the calcium bound to the endogenous mobile buffer. As only the number of free calcium ions and those attached to buffer within the 1 μm^3 volume are determined, spatial inhomogeneities in the concentration of these throughout the volume during the first few milliseconds after channel closure are not considered. Upon channel closure, there is a rapid decrease in free calcium (over microseconds), as it is bound principally to the fixed buffer (Fig. 6). Thereafter, the decline in free calcium is primarily due to the calcium ions released from

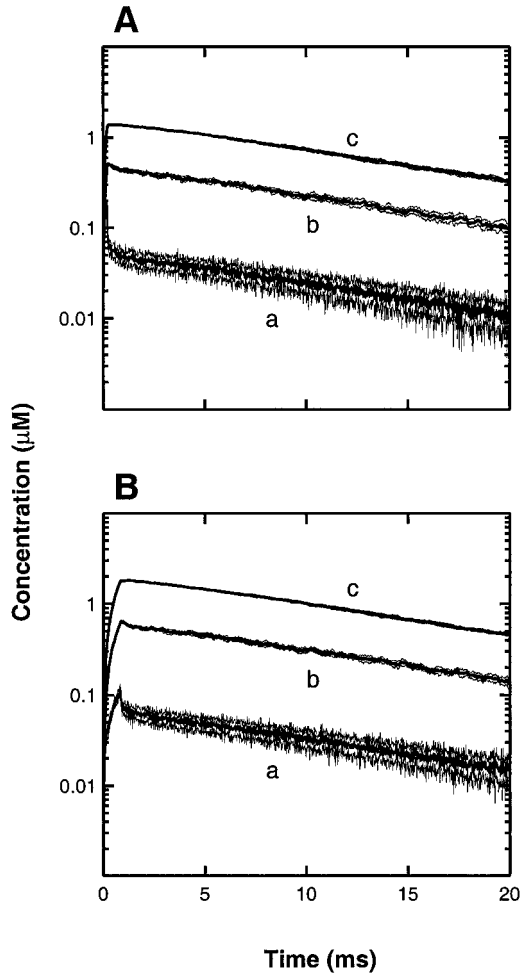

FIGURE 6 The mean and standard deviation of the calcium concentration in a cubic volume of 1 μm^3 about a single channel in a varicosity or bouton. The concentration is averaged over the whole cubic volume. (*A*) Results for the average spontaneous open time of an N-type channel of 0.2 ms with a current of 2 pA. (*B*) Results for the average evoked open time of an N-type channel of 0.84 ms with a current of 0.62 pA. In each case, curves *a–c* give the concentrations of free calcium ($[Ca^{2+}]$), of calcium bound to the mobile buffer ($[CaB_m]$), and the calcium bound to the fixed buffer ($[CaB_f]$), respectively. In each graph the heavy line shows the mean concentration (in μM) and the thin lines show one standard deviation away from the mean. Log ordinates.

the buffers finding the pumps on the walls of the 1 μm^3 volume. This free calcium falls to within 1/e of its initial value in ~15 ms (Fig. 6), a time that is mostly governed by the probability that once an ion hits the wall of the volume it will be extruded by a pump.

Effect of buffers and indicators on Ca^{2+}

The above calculations have all been made using the standard characteristics of the endogenous buffers given in Table 1. In this section consideration is given to the effects of varying the parameters of the mobile and fixed buffers as well as those of the indicator concentration when furaptra is used as the indicator. The case for which Monte Carlo simulations have been carried out is that of a spontaneously opening channel (0.8 ms and 2 pA), which gives the calcium transients in a varicosity or bouton of volume 1 μm^3 shown in Fig. 6. The temporal characteristics of the signal for calcium bound to furaptra, together with the peak free calcium transient, have been calculated in each case.

Fig. 7 shows the results of varying the characteristics of the mobile buffer and indicator on the time at half-peak of $[CaB_i]$ (Fig. 7, *A* and *B*). A 100-fold increase in $[B_m]_T$ produces only a threefold increase in the half-time of the $[CaB_i]$ signal (Fig. 7 *A*); similar increases in k_m^+ or K_m of the mobile buffer produce only about a twofold decrease in the half-time of the $[CaB_i]$ transient (Fig. 7 *A*). There is only a very small standard deviation about these mean values, so that they have not been included in the graph. Less than a threefold change occurs in the half-time of the $[CaB_i]$ as the result of a 100-fold increase in the values of $[B_i]_T$ and its k_i^+ or K_i values (Fig. 7 *B*); again there is very little variability associated with these values.

Fig. 8 shows the results in the case of varying the characteristics of the fixed buffer and indicator concentration on

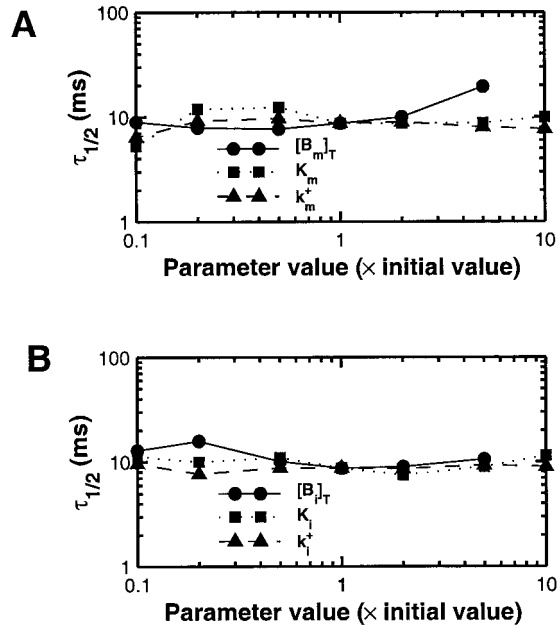

FIGURE 7 The effect of mobile buffer and indicator parameters on the half-time of the transient for calcium bound to the indicator furaptra ($[CaB_i]$), upon the opening of a spontaneous calcium channel (0.8 ms and 2 pA) in a bouton or varicosity of volume 1 $\mu m \times 1\ \mu m \times 1\ \mu m$. Results from Monte Carlo simulations are given for a range of parameter values for mobile buffer (B_m) and for indicator (B_i). (*A*) The parameter values of the mobile buffer ($[B_m]_T$; K_m; k_m^+) were changed while all other parameters were maintained at their standard values (Table 1). (*B*) The parameter values of the indicator ($[B_i]_T$; K_i; k_i^+) were changed while all other parameters were maintained at their standard values (Table 1). Calcium pumps were present in the walls of the volume under consideration, as outlined in the Methods section.

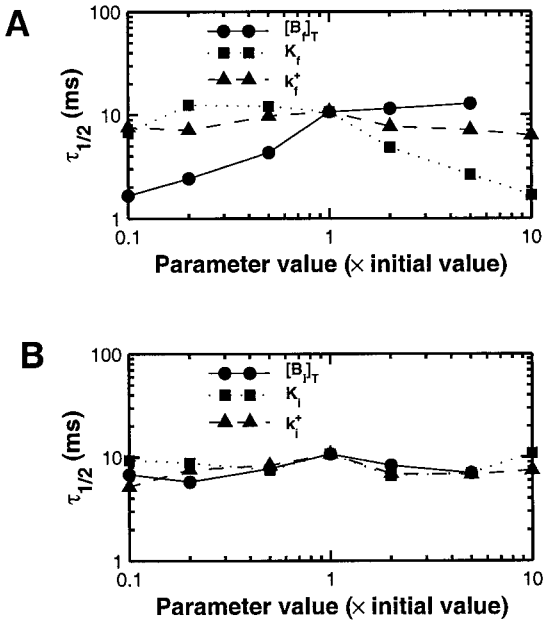

FIGURE 8 As for Fig. 7, except that the mobile buffer is now absent, and in (*A*) the parameter values of the fixed buffer are varied.

the time at half-peak of $[CaB_i]$ (Fig. 8, *A* and *B*). A 10-fold change in the values of $[B_f]_T$ and its k_f^+ can produce very significant changes (of the order of 10-fold), in the half-time of the $[CaB_i]$ transient, at the standard values for the B_m buffer and of furaptra given in Table 1; there is only a very small variation about these mean values (Fig. 8 *A*). There is only a small change in the half-time of the $[CaB_i]$ with a 100-fold change in the values of $[B_i]$, with again very little variation associated with these values, $[B_f]$ being kept at its standard value given in Table 1 (Fig. 8 *B*). These calculations show that the characteristics of the $[CaB_i]$ transient are relatively little affected by changes in the parameters of the mobile buffer or the indicator compared with changes in the fixed buffer parameters.

The effects of using furaptra or fura-2 as indicators on the calcium transients according to Monte Carlo simulations, for different properties of the endogenous buffers, are shown in Fig. 9 for the same conditions of opening of a calcium channel in a volume 1 μm^3. These were carried out for comparison with the deterministic calculations of Sinha et al. (1997) for a related model. (See the caption to Fig. 9 for the parameter choices corresponding to curves *a–d*.) The free calcium transient when furaptra is used as indicator is only slightly increased in amplitude and slowed if either the dissociation constant of the mobile buffer is increased (compare Fig. 9 *Ab* with *Aa*) or the mobile buffer is absent (compare Fig. 9 *Ac* with *Aa*). However, reducing the forward binding constant of the fixed buffer in the absence of mobile buffer greatly increases the amplitude of the free calcium transient without much change in its time course (compare Fig. 9 *Ad* with *Aa*).

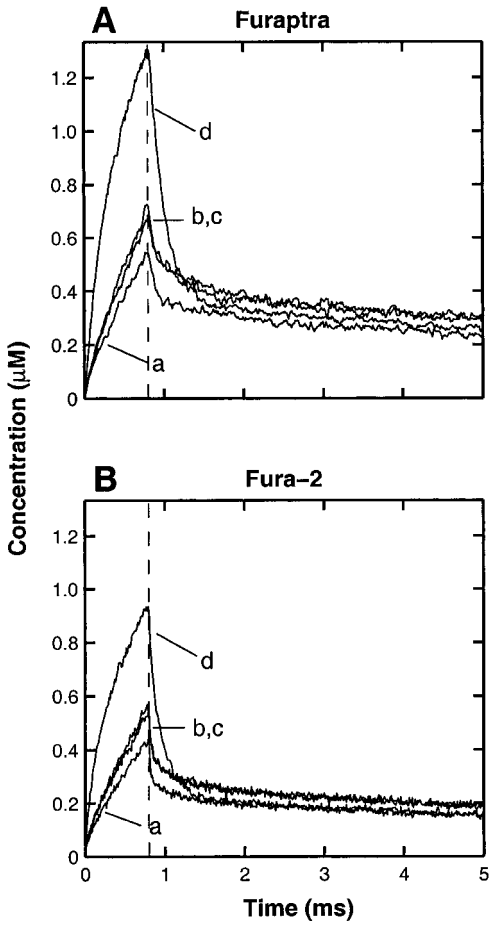

FIGURE 9 The effect of using furaptra (100 μM; *A*) or fura-2 (100 μM; *B*) as an indicator on the calcium transients calculated for different properties of the mobile and fixed buffers in a varicosity or bouton of 1 μm^3 upon the spontaneous opening of a calcium channel (0.8 ms and 2 pA); the vertical dashed line indicates the channel closing time. Shown are the free calcium concentrations, calculated as averages over the entire cubic volume. Four different sets of fixed and mobile buffer values were used: (*a*) $[B_m]_T$ and $[B_f]_T$ have the standard values given in Table 1; (*b*) as for (*a*), except that the dissociation constant of the mobile buffer is increased 10-fold; (*c*) $[B_m]_T$ is zero and $[B_f]_T$ has the standard value given in Table 1; (*d*) as for (*c*), except that the forward binding rate of the fixed buffer is reduced by a factor of 10. (Note that curves *b* and *c* are almost indistinguishable on the graph.)

Similar results are obtained if fura-2 is used as indicator (compare Fig. 9 *B* with *A*). It will be noted, however, that all of the calcium signals are faster in the presence of fura-2 compared with furaptra under all the conditions considered (compare Fig. 9 *B* with *A*). The average results given in Fig. 9 from the Monte Carlo simulations are qualitatively similar to those obtained in the deterministic modeling of Sinha et al. (1997; see their Fig. 7), except that there are substantial quantitative differences when considering the effects of removing the mobile buffer, which in the Monte Carlo simulations produces only a minor increase in the amplitude of the calcium transient compared with that in the calcula-

tion of Sinha et al. (1997). These differences are probably due to the very different geometry used by Sinha et al., namely a spherical terminal divided into homogeneous concentric shells.

Exocytosis due to a Ca^{2+}-microdomain: the secretory unit hypothesis

The secretory unit hypothesis supposes a complex formed between the calcium sensor vesicle-associated protein and a calcium channel. The distance between these has been variously placed as between 25 and 50 nm (see, for example, Stanley, 1993). In this section the effects on exocytosis of a single calcium channel opening at different distances from different spatial arrays of these calcium sensors plus their vesicles is determined for both spontaneous opening of the channel and the channel opening under an action potential.

Spontaneous channel opening

As before, the conditions of spontaneous opening are those for the average characteristics of an N-type channel (2 pA for 0.2 ms) and for a longer time of opening of such a channel (2 pA for 0.8 ms). In the first simulation, exocytosis has been considered from a secretory unit consisting of a single vesicle together with its calcium sensor protein (taken to be positioned at the center of the vesicle) with a calcium channel at different distances from the sensor (Fig. 10). The probability of exocytosis of a single vesicle in a secretory unit has been calculated for the case of the channel 25 nm from the calcium sensor protein (see Fig. 10, *Aa* and *Ab* for the 0.2 ms and 0.8 ms open times, respectively) or 50 nm from the sensor (see Fig. 10, *Ba* and *Bb* for the 0.2 ms and 0.8 ms open times, respectively). (Note that because there is only a single vesicle present, "mean quantal release" is identical to "probability of exocytosis.") The probability of exocytosis of the vesicle decreases by a factor of ~3 when the distance between the channel and the sensor increases from 25 to 50 nm in the case of the longer opening channel (compare Fig. 10, *Ab* and *Bb*). The results for the shorter opening channel are too small for a quantitative comparison (see Fig. 10, *Aa* and *Ba*). This latter observation is to be expected, as it has been shown above that for a given calcium influx the longer opening channels produce a higher concentration of calcium ions at the calcium sensor than do the shorter opening channels.

It is of interest to explore the effects of halving the single-channel current and of different schemes for calcium binding to the calcium sensor vesicle-associated protein on spontaneous quantal release at a single secretory unit. The probability of exocytosis of a single vesicle in a unit has been calculated for the case in which the channel is 25 nm from the calcium sensor protein and is open for 0.2 or 0.8 ms with a current of 1 pA for the following cases: standard binding rates for four binding sites on the sensor (Fig. 11, *Aa* and *Ab*, respectively); fast binding rates for four binding sites on the sensor (Fig. 11, *Ba* and *Bb*, respectively); fast binding rates for three binding sites only on the sensor (Fig. 11, *Ca* and *Cb*, respectively); fast binding rates for two binding sites on the sensor (Fig. 11, *Da* and *Db*, respectively). The probability of exocytosis of the vesicle is negligible for the short open times in all cases. For the longer openings the probability is nearly doubled, to ~0.10 or more when the binding rate is increased, and this occurred independent of whether four (Fig. 11 *Bb*), three (Fig. 11 *Cb*) or two (Fig.

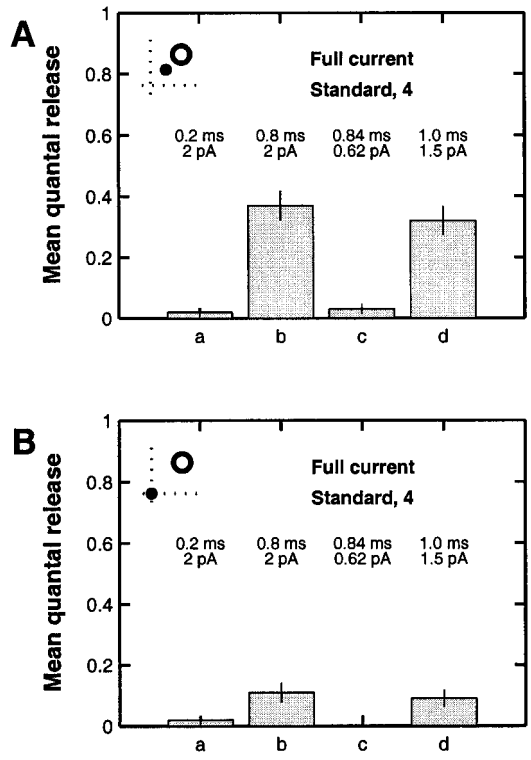

FIGURE 10 The dependence on calcium channel position of the mean number of exocytotic events (that is, mean quantal release) at a single secretory unit. The channel-vesicle distance is measured as the distance from the center of the N-type calcium channel to the center of the calcium sensor vesicle-associated protein, which is taken to be located at the site of anchoring of the vesicle to the presynaptic membrane. The binding scheme is given by Eq. 26 and "standard" values are used for the rates (Table 1). (*A*) Results for the case where the channel-vesicle distance is 25 nm (*inset*; where the channel is represented by a *small filled circle* and the vesicle by an *open circle*). (*B*) Results for the case where the channel-vesicle distance is 50 nm (*inset*). In each case, *a* and *b* correspond to spontaneous opening of the channel for 0.2 ms with 2 pA current and for 0.8 ms with 2 pA current, respectively; *c* and *d* correspond to evoked opening for 0.84 ms with 0.62 pA current and for 1.0 ms with 1.5 pA current, respectively. The bars give the mean of 100 Monte Carlo simulations and the vertical lines show the standard deviations for these 100 runs, calculated on the assumption that each release is an independent event with the same probability of occurrence p, where the mean is used as an estimate of p. (The release frequency thus follows a binomial distribution, with mean p and standard deviation $\sqrt{p(1-p)/n}$. For *Aa–Ad* the values of p are 0.02, 0.37, 0.03, and 0.32, respectively; for *Ba–Bd* they are 0.02, 0.11, 0.00, 0.09.) The parameters used in the calculations are given in Table 1.

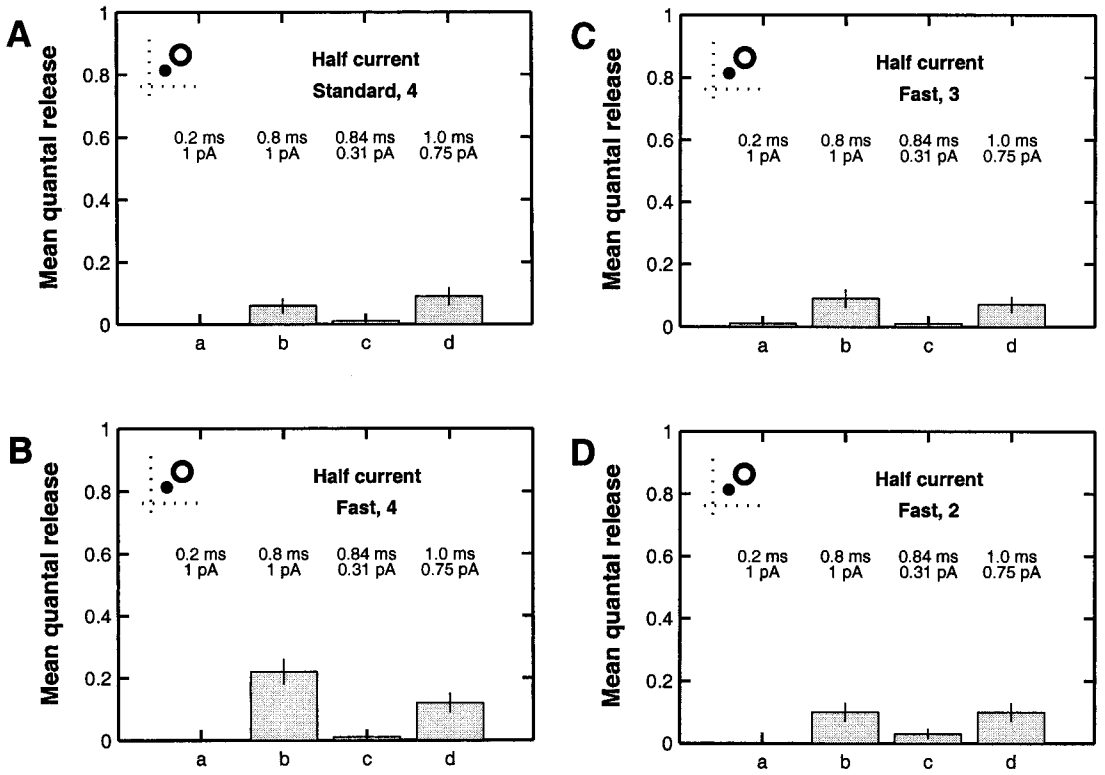

FIGURE 11 As for Fig. 10 *A*, except that the single-channel calcium current has been reduced to half the value used there and various different binding schemes are implemented. (*A*) four-binding case with "standard" rates (Table 1). (*B*) four-binding case with "fast" rates: $k^a = 14.3 \times 10^6\ M^{-1}\ s^{-1}$, $k^d = 130\ s^{-1}$, $\beta = 1000\ s^{-1}$. (*C*) three-binding case with "fast" rates: $k^a = 10.7 \times 10^6\ M^{-1}\ s^{-1}$, $k^d = 132\ s^{-1}$, $\beta = 1000\ s^{-1}$. (*D*) two-binding case with "fast" rates: $k^a = 6.4 \times 10^6\ M^{-1}\ s^{-1}$, $k^d = 129\ s^{-1}$, $\beta = 1000\ s^{-1}$. In these last three cases, the parameter values are from Heinemann et al. (1994).

11 *Db*) calcium binding sites existed in the calcium sensor. Further calculations showed that if the separation between the channel and the calcium sensor protein is increased to 50 nm, then the probability of release in all cases is reduced to <0.02.

The other configuration of vesicles and channels considered consists of an array of four vesicles at the corners of a square with 70.7-nm sides with a single calcium channel opening at different distances from one of the vesicles, as shown in Fig. 12. The mean quantal release from this array of vesicles has been calculated for the case of the channel 25 nm from the calcium sensor protein (see Fig. 12, *Aa* and *Ab* for the 0.2 ms and 0.8 ms open times, respectively) or 50 nm from the sensor (see Fig. 12, *Ba* and *Bb* for the 0.2 ms and 0.8 ms open times, respectively). The mean quantal release decreases by only 11% when the distance between the channel and the sensor increases from 25 to 50 nm, in the case of the longer opening channel (compare Fig. 12, *Ab* and *Bb*). As before, the results for the shorter opening channel are too small for a quantitative comparison (see Fig. 12, *Aa* and *Ba*). For the longer opening time there is multiquantal release on $\sim$10% of occasions that the channel opens for both 25- and 50-nm distances (Fig. 12, *Ab* and *Bb*), which together with the increase in single quantal release ensures that the average quantal release is greater for the four-vesicle case than the single-vesicle case (compare Fig. 12, *Aa* and *Ab* with Fig. 10, *Aa* and *Ab*; also compare Fig. 12, *Ba* and *Bb* with Fig. 10, *Ba* and *Bb*).

This stochastic analysis shows that the calcium entering through a channel may, for the long open time events and for vesicles clustered as in Fig. 12, occasionally reach vesicles that are $>$70 nm away and occupy the four binding sites on the calcium sensor necessary to trigger exocytosis. Thus multiquantal events can occur in which both the vesicle nearest the open channel and one much further away can undergo exocytosis when the vesicles are clustered (Fig. 12 *C*), a result that can only be revealed by a stochastic treatment.

Evoked channel opening

The conditions of opening of a calcium channel under an action potential are those determined previously for an N-type channel (0.84 ms and 0.62 pA) and for a longer time of opening of such a channel (1.0 ms and 1.5 pA). As for the spontaneous opening of a channel described above, exocytosis has been considered from a secretory unit consisting of a single vesicle together with its calcium sensor protein with

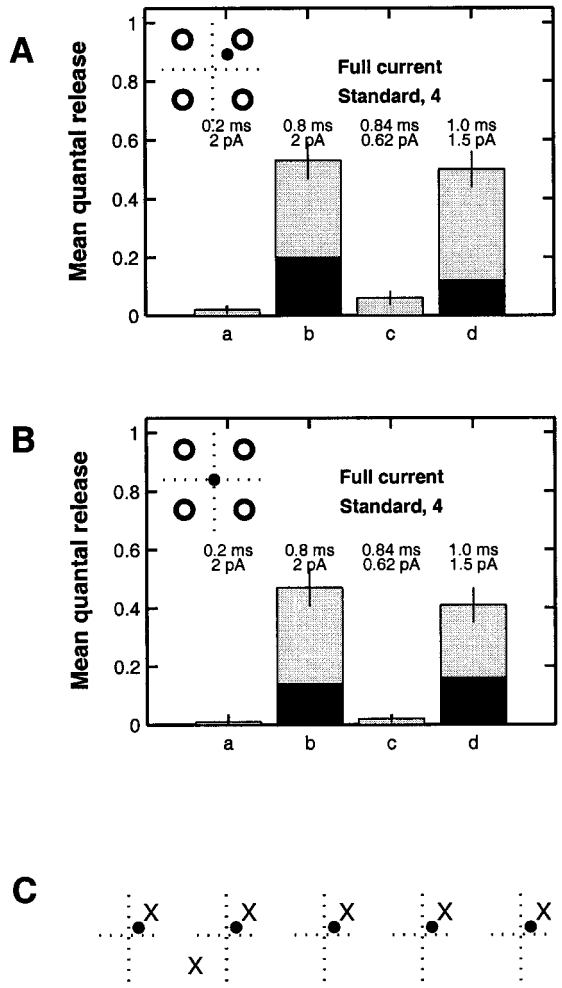

FIGURE 12 The dependence on calcium channel position of the mean number of exocytotic events at a set of secretory units in the case that only one of the channels opens. The channel-vesicle distance is measured as the distance from the N-type calcium channel to the calcium sensor vesicle-associated protein, which is taken to be located at the site of anchoring of the vesicle to the presynaptic membrane. Four vesicles are placed at the corners of a 70-nm square and only the channel associated with the upper right vesicle opens. (*A*) Results for the case where the channel-vesicle distance is 25 nm (*inset*) where the channel that opens is represented by a *small filled circle* and the vesicles by *open circles*). (*B*) Results for the case where the channel-vesicle distance is 50 nm (*inset*). In each case, panels *a* and *b* correspond to spontaneous opening of the channel for 0.2 ms with 2 pA current and for 0.8 ms with 2 pA current, respectively; panels *c* and *d* correspond to evoked opening for 0.84 ms with 0.62 pA current and for 1.0 ms with 1.5 pA current, respectively. The bars give the mean of 100 Monte Carlo simulations with the darker regions indicating the fraction due to two exocytotic events occurring, and the vertical lines show the standard deviations for these 100 runs. (*C*) A typical set of five cases in which exocytosis does occur (*crosses*) when the channel (*small filled circles*) is positioned as in (*A*), and opens for 0.8 ms with a 2 pA current. Standard deviations are calculated as for Fig. 10, except that in (*A*) a multinomial rather than a binomial distribution must be used, since the offset placing of the channel relative to the four vesicles means that all vesicles do not have the same probability of release. A four-binding scheme is used and all parameter values are as in Table 1.

a calcium channel at different distances from the sensor (Fig. 10). The probability of exocytosis of a single vesicle in a secretory unit has been calculated for the case of the channel 25 nm from the calcium sensor protein (see Fig. 10, *Ac* and *Ad* for the 0.84 and 1.5 ms open times, respectively) or 50 nm from the sensor (see Fig. 10, *Bc* and *Bd* for the 0.84 and 1.5 ms open times, respectively). The probability of exocytosis of the vesicle decreases by a factor of ~3 when the distance between the channel and the sensor increases from 25 to 50 nm in the case of the longer opening channel (compare Fig. 10, *Ad* and *Bd*). The results for the shorter opening channel are too small for a quantitative comparison (see Fig. 10, *Ac* and *Bc*).

The effects of halving the single-channel current and of different schemes for calcium binding to the sensor protein on evoked quantal release at a single secretory unit is shown in Fig. 11 (histograms *c* and *d*). The probability of exocytosis of a single vesicle in a unit has been calculated for the cases in which the channel is 25 nm from the calcium sensor and is open for 0.84 ms with a current of 0.31 pA (histogram *c* in Fig. 11), or for 1.0 ms with a current of 0.75 pA (histogram *d* in Fig. 11). The same cases were considered as for the spontaneous opening of the channel, namely: standard binding rates for four binding sites on the sensor (Fig. 11, *Ac* and *Ad*, respectively); fast binding rates for four binding sites on the sensor (Fig. 11, *Bc* and *Bd*, respectively); fast binding rates for three binding sites only on the sensor (Fig. 11, *Cc* and *Cd*, respectively); fast binding rates for two binding sites on the sensor (Fig. 11, *Dc* and *Dd*, respectively). The probability of exocytosis of the vesicle is small (<0.1) for the smaller current in all cases and is substantially increased for the longer current. Interestingly, the large current gives probabilities of ~0.1, independent of the different calcium binding schemes or of whether the binding rates are fast (Fig. 11, *Ad*, *Bd*, *Cd*, and *Dd*). These results showed that halving the current had an effect that is difficult to compensate for by increasing the binding rates or decreasing the number of binding sites on the calcium sensor molecule (compare Fig. 10, *Ad* with Fig. 11, *Ad*, *Bd*, *Cd*, and *Dd*).

The other configuration of vesicles and channels consists of an array of four vesicles at the corners of a 70-nm-side square, as described above (Fig. 12). The mean quantal release from this array of vesicles was then calculated for the case of the channel 25 nm from the calcium sensor protein (see Fig. 12, *Ac* and *Ad* for the 0.84 and 1.5 ms open times, respectively) or 50 nm from the sensor (see Fig. 12, *Bc* and *Bd* for the 0.84 and 1.5 ms open times, respectively). For the case of the shorter opening channel, the mean quantal release probability decreases considerably when the distance between the channel and the sensor increases from 25 to 50 nm (compare Fig. 12, *Ac* and *Bc*). For the longer opening times there is only a relatively small decrease in mean quantal release when the distance increases from 25 to 50 nm, with multiquantal release occurring on ~8% of

occasions on which the channel opens in both cases (Fig. 12, *Ad* and *Bd*).

A relatively high quantal release is thus common for the longer opening times. The stochastic analysis shows that calcium ions can on occasion reach the calcium sensors belonging to vesicles over 70 nm away from the open channel, in addition to the sensors within the secretory unit of the channel, if the channel is open for sufficient time. This does not happen for channels opening for shorter times. As previously shown, the longer time of calcium ion flux confers an advantage in that a sufficient number of ions in their random walk may reach the binding sites on a calcium sensor, at distances of the order of 70 nm, and then trigger exocytosis. This analysis shows then that secretory units may not act independently of each other when in an array of the kind shown in Fig. 12. Channels that open for relatively long times under an action potential can trigger exocytosis from secretory units other than the one in which they reside. The consequences of this lack of independence of secretory units on quantal release is considered in the next paper.

DISCUSSION

Monte Carlo method

The starting point for the present approach was the work of Bartol et al. (1991) who used a Monte Carlo method to study the diffusion and binding of transmitter in the neuromuscular junction. Subsequently, this method was used in a number of other investigations into transmitter action (Faber et al., 1992; Bennett et al., 1995b,c, 1996, 1997b). Most of these techniques can be taken over almost unchanged and applied to the diffusion and binding of calcium ions. The principal extensions that have to be made concern buffering and pumping.

The treatment used for the fixed buffer is basically the three-dimensional extension of Bartol et al.'s treatment of hydrolysis by acetylcholinesterase, which was assumed to lie in a two-dimensional sheet in the middle of the synaptic cleft. The treatment of the mobile buffer was more problematic and a special technique had to be developed, involving dividing the space into ~50-nm-sided cubes and assuming the number of bound plus free mobile buffer molecules remained constant in each cube (see Methods section). It is to be emphasized that this division into cubes was used for the mobile buffer only; the rest of the Monte Carlo simulation used the exact coordinates of the particles. The treatment of pumping through the terminal walls was also based on Bartol et al.'s approach to hydrolysis.

In the calcium case there is always present a background concentration of free calcium and of calcium bound to buffers, and this has no analog in the neurotransmitter case. The approach adopted here is to omit this background from the Monte Carlo simulation and to compensate for this omission by appropriate alteration of parameter values; this is justified by showing that the resulting errors are negligible.

The calculations were performed on a Digital Alpha 255/233 workstation. Simulations involving only a few thousand calcium ions took the order of minutes; simulations of facilitation under action potentials (to be reported in the following paper, Bennett et al., 2000) involved up to 100,000 calcium ions and took the order of one hour of computer time to follow the system for 15 ms of real time.

Parameter values

N-type channels were chosen for the modeling process, with the properties described in Delcour et al. (1993), as most of the synapses for which comparison was sought use these channels in the secretion process [namely the amphibian neuromuscular junction (Katz et al., 1995), the sympathetic neuromuscular junction (Wright and Angus, 1996), and autonomic preganglionic synapses (Haydon et al., 1994)]. The properties of N-type channels have only been studied to this time using Ba^{2+} as the charge carrier (Delcour et al., 1993). We have used, in some cases, a large channel current (2 pA) as this was necessary to obtain quantal release with the calcium affinities for the calcium sensor that have been published. However, we have also examined the effects of halving this current on the probability of exocytosis (Fig. 11). This has the effect of reducing both spontaneous and evoked release to very low levels for short-duration channel openings (compare Fig. 11 *A* with Fig. 10 *A*), using the standard affinity values. Such high levels of sensitivity of the release process to entering calcium have been observed directly at synapses formed between granule cells and Purkinje cells in the cerebellum (Sabatini and Regehr, 1997, 1998).

The calcium affinity values for the calcium sensor vesicle-associated protein were those best found to fit the experimental data for exocytosis from bipolar cells (Heidelberger et al., 1994) and from chromaffin cells (Heinemann et al., 1994). However, a range of other affinities have also been explored as well as the number of calcium binding sites on the sensor necessary to trigger exocytosis. In general, the effect of decreasing the current on the probability of evoked quantal release could not be compensated for by either increasing the binding rates of the sites on the calcium sensor or by decreasing the number of sites on the sensor that must be occupied by a calcium ion to trigger exocytosis. Thus the channel current is the critical factor in triggering exocytosis, besides that of the distance between the channel and synaptic vesicle.

The density σ_P of the calcium ATPase pump in the plasmalemma is ~2000 pumps per μm^2 according to the recent measurements for the membranes of the hair cell stereocilia (Yamoah et al., 1998), and this value has been used in the present calculations. Note, as already pointed out in the Methods section, that the precise value of σ_P is not

crucial, as the rate constants k_1 and k_2 are adjusted to compensate. The maximum pumping rate has been increased two orders of magnitude from the value of 3.2×10^{-13} mol cm^{-2} s^{-1} given for smooth muscle (Kargacin and Fay, 1991). This has been found necessary because if a lower rate is used, then calcium stays in the terminal. If the Kargacin and Fay (1991) value is used, then the calcium concentration does not decrease at all over 20 ms. Terminals are likely to have very high pumping rates (see Helmchen et al., 1997).

The estimate of the number of N-type calcium channels that open stochastically under a Hodgkin-Huxley action potential has been calculated at 46% of all the channels present (Bennett et al., 1997a), and this was used in the present work. Recently, direct measurement of this number in the calyx of Held revealed that ~69% of the channels opened (Borst and Sakmann, 1998).

Following Klingauf and Neher (1997), the diffusion coefficient for free calcium was taken as 220 μm s^{-1} for most calculations, this value being about one-third the value given for calcium diffusing in water (600–792 μm s^{-1}: see Winslow et al., 1994; Winslow, 1995). This reduction was to allow for the tortuosity and viscosity of the cytoplasm (see Kushmerick and Podolsky, 1969). However, we have also done additional calculations using a higher calcium diffusion coefficient (792 μm s^{-1}). The effect is to significantly decrease the amount of free calcium within ~30 nm of a channel at the time of its closing; the amount of calcium bound to the fixed buffer within ~200 nm of the channel mouth is also somewhat decreased, but the amount bound to the mobile buffer is almost unchanged, with the escaped calcium binding to fixed buffers at distances of 100 nm or more from the channel. The effect of this is to reduce the probability of exocytosis.

Calcium in the microdomain about a single open channel

The dynamics of calcium movement at sites of regulated secretion have been intensively studied using deterministic solutions to the diffusion equations and the kinetic equations describing the reaction of calcium with the endogenous buffers and exogenous indicators (Neher, 1995). A stochastic analysis of these dynamics has been carried out in the present work, using Monte Carlo simulations, as the process of secretion is stochastic so that the underlying mechanisms responsible for secretion have to be examined using a probabilistic approach. It has generally been taken for granted that the number of calcium ions that enter through a calcium channel is so large that deterministic solutions are adequate to describe their dynamics (Naraghi and Neher, 1997). The present work shows that this is not the case for the deterministic opening of a single channel when distances from the channel mouth are considered that are likely to contain the calcium sensor for triggering exocytosis, that is, within ~50 nm. In this case the fluctuations in the number of calcium ions are such that the standard deviation is about half the mean. These stochastic fluctuations are not described by the deterministic equations that give the buffered diffusion of calcium in the presence of relatively rapid fixed and mobile buffers near an open channel (Wagner and Keizer, 1994; Smith, 1996), although the mean number of calcium ions near the channel is well-described by these equations (see Fig. 5).

Naraghi and Neher (1997) have recently provided a linearized approximation of the combined diffusion and reaction of calcium with mobile buffer near an open channel (see also Pape et al., 1995). This approximation cannot be used in the present work as it only holds away from buffer saturation, a condition that is not met in these studies (see Fig. 5 *A* for comparisons). Nevertheless, neither the deterministic solutions provided by the linearized approximations nor the rapid buffering approximations can provide the insights into the calcium fluctuations near the channel mouth that are given by the Monte Carlo calculations. The present work shows that the mean number of calcium ions within 10 nm of the mouth of the channels that pass the currents and open for the times considered representative of spontaneous openings and evoked openings is such as to give rise to concentrations there of the order of 100 μM at the end of the channel opening. However, one should note that a concentration of 100 μM means that only an average of 0.126 calcium ions is in a hemispherical volume of radius 10 nm. This emphasizes the stochastic nature of these processes and provides further justification for adopting a Monte Carlo approach. At that time the concentration declines along several characteristic length constants with a dominant one at ~100 nm.

The microdomains generated in this Monte Carlo analysis are different from those calculated, using deterministic equations, by Aharon et al. (1994) and Simon and Llinás (1985). In the former case, tail currents for the calcium influx were arbitrarily chosen to be of 0.1 ms duration. In addition, equilibrium equations were used to describe a decreased calcium influx attributed to an increased calcium concentration at the inside mouth of the channel. This kind of model gave rise to high concentrations within very small distances from the channel. Simon and Llinás (1985) also find calcium domain of small spatial extent in their calculations, but they use a value for the dissociation constant of the mobile buffer that is one to two orders of magnitude smaller than the one used in the present calculations.

Calcium in a varicosity or bouton after the opening of a single channel

The characteristics expected for the calcium transient after the opening of a single calcium channel in small boutons and varicosities, of the order of 1 μm diameter, were determined. A similar problem has been examined by Sinha et

al. (1997) by solving the deterministic equations for the diffusion and buffer reactions together with that for a plasmalemma calcium pump. Although they considered radial symmetry, in which calcium enters around the entire periphery of the bouton, this calcium amounted to 1 pA for 1 ms, and therefore was about the same as the flux of calcium ions considered in the present calculations as passing through a single channel. Their results for the half-decay time of the low-affinity furaptra indicator signal were similar to those obtained with the average in the Monte Carlo simulation, namely between 10 and 20 ms (compare their Fig. 5 with Fig. 7). The same model has been used for the calciform terminal in the nucleus of Held to obtain an exponential decay of ~45 ms (Helmchen et al., 1997). These temporal characteristics of the furaptra transient only change about threefold for several orders of magnitude change in the concentration and kinetic parameters of the mobile buffer, while the amplitude of the transient does not decrease with an increase in the concentration of such an indicator until ~100 μM. Similar qualitative trends were observed in the deterministic modeling of Sinha et al. (1997; see their Fig. 5) also see Tank et al. (1995).

Quantal release at calcium microdomains

Both the duration of the open time of the calcium channel and its position with respect to the calcium sensor in the secretory unit determine the probability of exocytosis of the vesicle in the secretory unit, as these determine the probability that sufficient calcium ions reach the sensor (Bennett et al., 1997a). The Monte Carlo simulations show that for a twofold increase in the distance there is a threefold decrease in the probability of secretion over the range of 25 to 50 nm for longer opening channels. Stochastic analysis of the case in which four secretory units are in a rectangular array, similar to that observed at some very small active zones in crayfish motor-nerve terminals (Cooper et al., 1996), shows that there is ~12% multiquantal release on the opening of a single channel for relatively long times, even though a vesicle may be separated from the channel by 100 nm. This multiquantal release would not be anticipated on the basis of a deterministic solution of the reaction-diffusion equations for calcium dynamics as it is in the case of stochastic solutions (Bennett et al., 1995a). It indicates that secretory units are unlikely to act independently of each other if they are arranged in rectangular arrays, and action potentials open about half the channels passing relatively high calcium currents, some of which will have relatively long open times.

When secretory units are arranged in a line, as in the active zone of motor-nerve terminals, the present results suggest that they also may not act independently of each other if they are separated by distances up to ~70 nm. The following paper (Bennett et al., 2000) investigates more completely the question of the interaction between secretory units when they are arranged in different arrays in the active zone of nerve terminals and an action potential triggers the opening of calcium channels.

APPENDIX A: BUFFERING APPROXIMATIONS

Time scale for buffering

To establish the validity of the rapid buffering approximation it is desirable to have an estimate of the time necessary for the buffers to reach equilibrium. This can be found by linearizing the buffer equations about their equilibrium points.

Because the buffer time will turn out to be much faster than the characteristic time for diffusion, for the purposes of this analysis the diffusion term can be omitted from Eq. 6, and Eqs. 6 and 8 can both be written as (where i is f or m)

$$\frac{d[\mathrm{CaB_i}]}{dt} = k^+[\mathrm{Ca^{2+}}][\mathrm{B_i}] - k^-[\mathrm{CaB_i}]. \tag{30}$$

Now $[\mathrm{B_i}] + [\mathrm{CaB_i}] = [\mathrm{B_i}]_\mathrm{T}$ and $[\mathrm{Ca^{2+}}] + [\mathrm{CaB_i}] = [\mathrm{Ca^{2+}}]_\mathrm{T}$, where subscript T denotes total initial amount. Thus Eq. 30 can be recast in the form

$$\frac{dX}{dt} = k^+X^2 - \alpha X + \beta \equiv f(X), \tag{31}$$

where $X = [\mathrm{CaB_i}]$, $\alpha = k^+([\mathrm{B_i}]_\mathrm{T} + [\mathrm{Ca^{2+}}]_\mathrm{T}) + k^-$, and $\beta = k^+[\mathrm{B_i}]_\mathrm{T}[\mathrm{Ca^{2+}}]_\mathrm{T}$. From Eq. 31 there is a stable equilibrium point at $X = X_\mathrm{e} = (\alpha - \sqrt{\alpha^2 - 4k^+\beta})/2k^+$, and linearizing about this point shows that the system approaches equilibrium with a time constant

$$\tau = 1/f'(X_\mathrm{e}) = 1/\sqrt{\alpha^2 - 4k^+\beta}. \tag{32}$$

This can be re-expressed in terms of equilibrium values as $\tau = 1/[k^- + k^+([\mathrm{Ca^{2+}}]_\mathrm{e} + [\mathrm{B_i}]_\mathrm{e})]$, which agrees with Wagner and Keizer (1994), Eq. 20. However, the initial value expression (Eq. 32) is more convenient for actual calculation.

From Eq. 32,

$$\tau = \frac{1}{\sqrt{(k^+)^2([\mathrm{B_i}]_\mathrm{T} - [\mathrm{Ca^{2+}}]_\mathrm{T})^2 + (k^-)^2 + 2k^-k^+([\mathrm{B_i}]_\mathrm{T} + [\mathrm{Ca^{2+}}]_\mathrm{T})}}$$

$$\leq \frac{1}{\sqrt{(k^-)^2 + 2k^-k^+[\mathrm{B_i}]_\mathrm{T}}}, \tag{33}$$

giving an upper bound on τ, regardless of the initial calcium concentration. For the values given in Table 1 this gives upper bounds of 25.6 μs for the fixed buffer, 43.6 μs for the mobile buffer, 288 μs for fura-2, and 16 μs for furaptra. Inclusion of an initial calcium concentration will reduce these estimates. These are thus much shorter than diffusion times, which are typically of the order of 5 ms for a distance of 1 μm.

Background calcium and buffering

In the Monte Carlo method it is assumed that the buffer molecules that are bound to the background calcium remain bound and do not enter into the calculations; in addition, only calcium ions in excess of the background are used in the simulation. We investigate the error introduced by this approximation.

For buffer i, the rapid buffering approximation gives (cf. Eq. 9)

$$[\mathrm{CaB_i}]_{\mathrm{actual}} = \frac{[\mathrm{Ca^{2+}}]_{\mathrm{actual}}[\mathrm{B_i}]_{\mathrm{T}}}{K_{\mathrm{i}} + [\mathrm{Ca^{2+}}]_{\mathrm{actual}}}, \tag{34}$$

where the subscript "actual" means that the background is included. If the background is not included the rapid buffering approximation now gives

$$[\mathrm{CaB_i}]_{\mathrm{excess}} = \frac{[\mathrm{Ca^{2+}}]_{\mathrm{excess}}[\mathrm{B_i}]_{\mathrm{excess}}}{K_{\mathrm{i}} + [\mathrm{Ca^{2+}}]_{\mathrm{excess}}}, \tag{35}$$

where $[\mathrm{CaB_i}]_{\mathrm{excess}}$ denotes bound buffer molecules in excess of those bound to background calcium, $[\mathrm{B_i}]_{\mathrm{excess}}$ is given by Eq. 16 with $f \rightarrow i$ and $[\mathrm{Ca^{2+}}]_{\mathrm{excess}}$ by Eq. 15. Thus the Monte Carlo scheme approximates the true bound buffer concentration by

$$[\mathrm{CaB_i}]_{\mathrm{approx}} = [\mathrm{CaB_i}]_{\mathrm{background}} + [\mathrm{CaB_i}]_{\mathrm{excess}}, \tag{36}$$

where $[\mathrm{CaB_i}]_{\mathrm{background}} = [\mathrm{B_i}]_{\mathrm{T}} - [\mathrm{B_i}]_{\mathrm{excess}}$ is the concentration of buffer bound to background calcium. Using Eq. 35 this is

$$[\mathrm{CaB_i}]_{\mathrm{approx}} = [\mathrm{B_i}]_{\mathrm{T}} - \frac{K_{\mathrm{i}}[\mathrm{B_i}]_{\mathrm{excess}}}{K_{\mathrm{i}} + [\mathrm{Ca^{2+}}]_{\mathrm{excess}}}. \tag{37}$$

The relative error involved is $\mathscr{E} = ([\mathrm{CaB_i}]_{\mathrm{approx}} - [\mathrm{CaB_i}]_{\mathrm{actual}})/[\mathrm{CaB_i}]_{\mathrm{actual}}$. Using Eqs. 16, 34, and 37, this is

$$\mathscr{E} = \frac{K_{\mathrm{i}}c_0(x - c_0)}{(K_{\mathrm{i}} + c_0)x(K_{\mathrm{i}} + x - c_0)}, \tag{38}$$

where $x = [\mathrm{Ca^{2+}}]_{\mathrm{actual}}$. This error has a maximum value

$$\mathscr{E}_{\max} = \frac{K_{\mathrm{i}}c_0}{(K_{\mathrm{i}} + c_0)(\sqrt{K_{\mathrm{i}}} + \sqrt{c_0})^2}, \tag{39}$$

when $x = c_0 + \sqrt{c_0 K_{\mathrm{i}}}$.

For the fixed and the mobile endogenous buffers, the parameter values in Table 1 give $\mathscr{E}_{\max} = 0.0082$ when $x = 1.1\ \mu$M. For furaptra $\mathscr{E}_{\max} = 0.0015$ when $x = 2.55\ \mu$M. Only for fura-2 is the error significant ($\mathscr{E}_{\max} = 0.109$) but this maximum occurs at a very low concentration ($x = 0.26\ \mu$M); for higher concentrations the error decreases rapidly, being $<2\%$ for calcium concentrations $>2.5\ \mu$M.

APPENDIX B: PSEUDO-CODE FOR MONTE CARLO SCHEME

```
MAIN
Preset input options
Seed random number generator
Loop over different runs
  Read data
  Open output files
  Select standard set of parameters
  Setup run using standard parameters modified by
  input data (SETUP)
  Initialize random displacements
  Loop over time
   Change number of active Ca ions to simulate
   delayed release, taking into account number of
   channels, number of pulses, current time, etc.
   Move the active Ca ions (MOVEP)
   Check for random exocytosis of fully bound
   receptors
    If passes test, flag receptor now out of
    model, and flag Ca ions out of model.
    Increment time
    Write output—number of Ca ions and receptors in
    each state (bound, free, exocytosed etc).
    Option of dumping the positions of all Ca ions
    at selected times.
  End loop over time
  Close files
End loop over runs
STOP
************************************************
SETUP
Determine diffusion constants (Ca, mobile buffer,
indicator)
Compute diffusion lengths—sqrt (4 D dt / pi)
Determine receptor density and size
Calculate receptor tile size—1/sqrt(density)

Determine buffer and indicator total
concentrations (bound and unbound).
Calculate block size (edge of cube) for fixed
buffer—1/cuberoot(conc)

Set geometry
  Determine size of model (change the width of the
  model to an exact number of receptor tiles, and
  the depth to an exact number of buffer blocks).
Set receptor structure
Flag receptor tiles as active or not, and no
calcium bound to them.

Set pump tiling
  Determine required density of pumps. (The size
  of the tiles is set so that exact number fit
  along each side of model.)
Flag all pump tiles as active with no calcium
bound.

Set fixed buffer structure
Flag all buffers blocks as active with no calcium
bound.

Determine stoichiometry and rate constants of
binding of calcium to receptor.
Calculate binding probabilities (p_off = k_off
dt, p_on = k_on * sqrt(pi dt / D_Ca) / (pi
radius^ 2) where radius is active size of receptor
(ie not full tile) )

Determine rate constants for final exocytosis of
fully bound receptor
Calculate probability (k_open dt)

Determine background calcium concentration
Convert to count of free ions.

Determine rate constants for binding to buffers
and indicator
Calculate equilibrium constants K_d for buffers
and indicator
Calculate background concentration of free mobile
buffer and indicator (c = c_total/(1 + Ca_0/K_d))
Calculate binding probabilities (p_off = k_off
dt, p_on = k_on dt c_mobile. p_on = k_on dt /
(tile size^ 3) for fixed buffer)

Set up nested domains for mobile buffer and
indicator
  The concentrations of mobile buffer and
  indicator are adjusted so that an integer number
  of molecules are found in each domain. The
  number of free molecules is initialized equal to
```

```
  the total number of molecules.
Determine constants for operation of pumps.
Calculate binding probabilities (p_on = rate *
sqrt(pi dt / D_Ca) / c_pump, p_off = rate dt
(tile area))
Adjust probabilities to allow for background
calcium (p_on = p_on * [c_pump( K_pump +
Ca_0)]^ 2, p_off = p_off * c_pump( K_pump +
Ca_0))
Bind background level of calcium to fixed buffer.
(Fraction is Ca_0/(Ca_0 + Kd))
Calculate total number of calcium ions, given
currents and numbers of channels.
Set up coordinates of release points, and table of
times for release.
RETURN
************************************************
MOVEP
Loop over active Ca ions
  CASE
  Pumped out:
   do nothing
  Disappeared in exocytosis:
   do nothing
  Disappeared beyond edge of model (in case where
  not completely enclosed):
   do nothing
  Bound to receptor:
   check for random unbinding, if passes test then
    flag Ca now free
    flag receptor has one less Ca
  Bound to fixed buffer:
   check for random unbinding, if passes test then
    flag Ca now free
    flag buffer is now unbound
  Bound to mobile buffer:
   check for random unbinding
    if passes test then flag Ca now free
    otherwise randomly displace the Ca/buffer,
    allowing for reflection off walls. If changes
    domain, adjust the probabilities within the
    domains.
  Bound to indicator:
   check for random unbinding
    if passes test then flag Ca now free
    otherwise randomly displace the Ca/indicator
  Bound to pump:
   check for random unbinding, if passes test then
    flag Ca now pumped out
    flag pump is now unbound
  Free calcium:
   Randomly displace the Ca ion, allowing for
   reflection off walls. If hits a wall, need to
   consider whether any binding occurs.
    case of receptor tile, must hit central disc,
    and receptor must not be fully bound or have
    undergone exocytosis.
   CASE
   Bind to receptor:
    flag Ca now bound
    increment Ca count on receptor
   Binds to pump:
    flag Ca now bound
    flag pump now bound
  Still free:
   Check for random binding to buffers/indicator
   in the case of fixed buffer, can only bind to
   free buffer sites
       in the case of mobile buffer and
       indicator, probability depends on current
       domain parameters
       CASE
       Binds to fixed buffer:
        flag Ca now bound
        flag buffer now bound
       Binds to mobile buffer:
        flag Ca now bound
        adjust the domain probabilities
       Binds to indicator:
        flag Ca now bound
        adjust the domain probabilities
       ENDCASE
     ENDCASE
   ENDCASE
  End loop over active Ca ions
  RETURN
```

This work was supported by an Australian Research Council Institutional Grant.

REFERENCES

Aharon, S., H. Parnas, and I. Parnas. 1994. The magnitude and significance of Ca^{2+} domains for release of neurotransmitter. *Bull. Math. Biol.* 56:1095–1119.

Augustine, G. J., E. M. Adler, and M. P. Charlton. 1991. The calcium signal for transmitter secretion from presynaptic nerve terminals. *Ann. NY Acad. Sci.* 635:365–381.

Bartol, T. M., Jr., B. R. Land, E. E. Salpeter, and M. M. Salpeter. 1991. Monte Carlo simulation of miniature endplate current generation in the vertebrate neuromuscular junction. *Biophys. J.* 59:1290–1307.

Bennett, M. R. 1996. Neuromuscular transmission at an active zone: the secretosome hypothesis. *J. Neurocytol.* 25:869–891.

Bennett, M. R., L. Farnell, and W. G. Gibson. 1995b. Quantal transmission at purinergic synapses: stochastic interaction between ATP and its receptors. *J. Theor. Biol.* 175:397–404.

Bennett, M. R., L. Farnell, and W. G. Gibson. 1996. Quantal transmitter release at somatic motor-nerve terminals: stochastic analysis of the subunit hypothesis. *Biophys. J.* 70:654–668.

Bennett, M. R., L. Farnell, and W. G. Gibson. 1998. On the origin of skewed distributions of spontaneous synaptic potentials in autonomic ganglia. *Proc. R. Soc. Lond. B.* 265:271–277.

Bennett, M. R., L. Farnell, and W. G. Gibson. 2000. The probability of quantal secretion within an array of calcium channels of an active zone. *Biophys. J.* 78:2222–2240.

Bennett, M. R., L. Farnell, W. G. Gibson, and S. Karunanithi. 1995c. Quantal transmission at purinergic junctions: stochastic interaction between ATP and its receptors. *Biophys. J.* 68:925–935.

Bennett, M. R., L. Farnell, W. G. Gibson, and N. A. Lavidis. 1997b. Synaptic transmission at visualized sympathetic boutons: stochastic interaction between acetylcholine and its receptors. *Biophys. J.* 72: 1595–1606.

Bennett, M. R., W. G. Gibson, and J. Robinson. 1995a. Probabilistic secretion of quanta: spontaneous release at active zones of varicosities, boutons, and endplates. *Biophys. J.* 69:42–56.

Bennett, M. R., W. G. Gibson, and J. Robinson. 1997a. Probabilistic secretion of quanta and the synaptosecretosome hypothesis: evoked release at active zones of varicosities, boutons, and endplates. *Biophys. J.* 73:1815–1829.

Borst, J. G., and B. Sakmann. 1998. Calcium current during a single action potential in a large presynaptic terminal of the rat brainstem. *J. Physiol.* 506:143–157.

Brose, N., A. G. Petrenko, T. C. Südhof, and R. Jahn. 1992. Synaptotagmin: a calcium sensor on the synaptic vesicle surface. *Science.* 256:1021–1025.

Clay, J. R., and L. J. DeFelice. 1983. Relationship between membrane excitability and single channel open-close kinetics. *Biophys. J.* 42: 151–157.

Cooper, R. L., J. L. Winslow, C. K. Govind, and H. L. Atwood. 1996. Synaptic structural complexity as a factor enhancing probability of calcium-mediated transmitter release. *J. Neurophysiol.* 75:2451–2466.

Delcour, A. H., D. Lipscombe, and R. W. Tsien. 1993. Multiple modes of N-type calcium channel activity distinguished by differences in gating kinetics. *J. Neurosci.* 13:181–194.

el Far, O., N. Charvin, C. Leveque, N. Martin-Moutot, M. Takahashi, and M. J. Seagar. 1995. Interaction of synaptobrevin (VAMP)-syntaxin complex with presynaptic calcium channels. *FEBS Lett.* 361:101–105.

Faber, D. S., W. S. Young, P. Legendre, and H. Korn. 1992. Intrinsic quantal variability due to stochastic properties of receptor-transmitter interactions. *Science.* 258:1494–1498.

Haydon, P. G., E. Henderson, and E. F. Stanley. 1994. Localization of individual calcium channels at the release face of a presynaptic nerve terminal. *Neuron.* 13:1275–1280.

Heidelberger, R., C. Heinemann, E. Neher, and G. Matthews. 1994. Calcium dependence of the rate of exocytosis in a synaptic terminal. *Nature.* 371:513–515.

Heinemann, C., R. H. Chow, E. Neher, and R. S. Zucker. 1994. Kinetics of the secretory response in bovine chromaffin cells following flash photolysis of caged Ca^{2+}. *Biophys. J.* 67:2546–2557.

Heinemann, C., L. von Rüden, R. H. Chow, and E. Neher. 1993. A two-step model of secretion control in neuroendocrine cells. *Pflügers Arch. Eur. J. Physiol.* 424:105–112.

Helmchen, F., J. G. Borst, and B. Sakmann. 1997. Calcium dynamics associated with a single action potential in a CNS presynaptic terminal. *Biophys. J.* 72:1458–1471.

Kargacin, G., and F. S. Fay. 1991. Ca^{2+} movement in smooth muscle cells studied with one- and two-dimensional diffusion models. *Biophys. J.* 60:1088–1100.

Katz, B., P. A. Ferro, B. D. Cherksey, M. Sugimori, R. Llinás, and O. D. Uchitel. 1995. Effect of Ca^{2+} channel blockers on transmitter release and presynaptic currents at the frog neuromuscular junction. *J. Physiol.* 486:695–706.

Klingauf, J., and E. Neher. 1997. Modeling buffered Ca^{2+} diffusion near the membrane: implications for secretion in neuroendocrine cells. *Biophys. J.* 72:674–690.

Kushmerick, M. J., and R. J. Podolsky. 1969. Ionic mobility in muscle cells. *Science.* 166:1297–1298.

Martin-Moutot, N., N. Charvin, C. Leveque, K. Sato, T. Nishiki, S. Kozaki, M. Takahashi, and M. Seagar. 1996. Interaction of SNARE complexes with P/Q-type calcium channels in rat cerebellar synaptosomes. *J. Biol. Chem.* 271:6567–6570.

Murray, J. D. 1993. Mathematical Biology. Springer, Berlin.

Naraghi, M., and E. Neher. 1997. Linearized buffered Ca^{2+} diffusion in microdomains and its implications for calculation of $[Ca^{2+}]$ at the mouth of a calcium channel. *J. Neurosci.* 17:6961–6973.

Neher, E. 1995. The use of fura-2 for estimating Ca buffers and Ca fluxes. *Neuropharmacol.* 34:1423–1442.

Neher, E. 1986. Concentration profiles of intracellular calcium in the presence of a diffusible chelator. *In* Calcium Electrogenesis and Neuronal Functioning. U. Heinemann, M. Klee, E. Neher, and W. Singer, editors. Springer, Berlin. 80–96.

Nowycky, M. C., and M. J. Pinter. 1993. Time courses of calcium and calcium-based buffers following calcium influx in a model cell. *Biophys. J.* 64:77–91.

O'Connor, V. M., O. Shamotienko, E. Grishin, and H. Betz. 1993. On the structure of the "synaptosecretosome." Evidence for a neurexin/synaptotagmin/syntaxin/Ca^{2+} channel complex. *FEBS Lett.* 326:255–260.

Pape, P. C., D. S. Jong, and W. K. Chandler. 1995. Calcium release and its voltage dependence in frog cut muscle fibers equilibrated with 20 mM EGTA. *J. Gen. Physiol.* 106:259–336.

Press, W. H., B. P. Flannery, S. A. Teukolsky, and W. T. Vetterling. 1989. Numerical Recipes: The Art of Scientific Computing. Cambridge University Press, Cambridge.

Rettig, J., C. Heinemann, U. Ashery, Z. H. Sheng, C. T. Yokoyama, W. A. Catterall, and E. Neher. 1997. Alteration of Ca^{2+} dependence of neurotransmitter release by disruption of Ca^{2+} channel/syntaxin interaction. *J. Neurosci.* 17:6647–6656.

Robitaille, R., M. L. Garcia, G. J. Kaczorowski, and M. P. Charlton. 1993. Functional colocalization of calcium and calcium-gated potassium channels in control of transmitter release. *Neuron.* 11:645–655.

Sabatini, B. L., and W. G. Regehr. 1997. Control of neurotransmitter release by presynaptic waveform at the granule cell to Purkinje cell synapse. *J. Neurosci.* 17:3425–3435.

Sabatini, B. L., and W. G. Regehr. 1998. Optical measurement of presynaptic calcium currents. *Biophys. J.* 74:1549–1563.

Sala, F., and A. Hernandez-Cruz. 1990. Calcium diffusion modeling in a spherical neuron. Relevance of buffering properties. *Biophys. J.* 57: 313–324.

Simon, S. M., and R. R. Llinás. 1985. Compartmentalization of the submembrane calcium activity during calcium influx and its significance in transmitter release. *Biophys. J.* 48:485–498.

Sinha, S. R., L. G. Wu, and P. Saggau. 1997. Presynaptic calcium dynamics and transmitter release evoked by single action potentials at mammalian central synapses. *Biophys. J.* 72:637–651.

Smith, G. D. 1996. Analytical steady-state solution to the rapid buffering approximation near an open Ca^{2+} channel. *Biophys. J.* 71:3064–3072.

Smith, G. D., J. Wagner, and J. Keizer. 1996. Validity of the rapid buffering approximation near a point source of calcium ions. *Biophys. J.* 70:2527–2539.

Stanley, E. F. 1993. Single calcium channels and acetylcholine release at a presynaptic nerve terminal. *Neuron.* 11:1007–1011.

Stern, M. D. 1992. Buffering of calcium in the vicinity of a calcium pore. *Cell Calcium.* 13:183–192.

Südhof, T. C. 1995. The synaptic vesicle cycle: a cascade of protein-protein interactions. *Nature.* 375:645–653.

Tank, D. W., W. G. Regehr, and K. R. Delaney. 1995. A quantitative analysis of presynaptic calcium dynamics that contribute to short-term enhancement. *J. Neurosci.* 15:7940–7952.

Wagner, J., and J. Keizer. 1994. Effects of rapid buffers on Ca^{2+} diffusion and Ca^{2+} oscillations. *Biophys. J.* 67:447–456.

Winslow, J. L. 1995. Apparent diffusion coefficient estimation errors from using ration of bound to unbound Ca^{2+}. *In* The Neurobiology of Computation. J. M. Bower, editor. 33–38. Kluwer Academic Publishers, Boston.

Winslow, J. L., S. N. Duffy, and M. P. Charlton. 1994. Homosynaptic facilitation of transmitter release in crayfish is not affected by mobile calcium chelators: implications for the residual ionized calcium hypothesis from electrophysiological and computational analyses. *J. Neurophysiol.* 72:1769–1793.

Wright, C. E., and J. A. Angus. 1996. Effects of N-, P- and Q-type neuronal calcium channel antagonists on mammalian peripheral neurotransmission. *Br. J. Pharmacol.* 119:49–56.

Yamoah, E. N., E. A. Lumpkin, R. A. Dumont, P. J. Smith, A. D. Hudspeth, and P. G. Gillespie. 1998. Plasma membrane Ca^{2+}-ATPase extrudes Ca^{2+} from hair cell stereocilia. *J. Neurosci.* 18:610–624.

Yoshida, A., C. Oho, A. Omore, R. Kuwahara, T. Ito, and M. Takahashi. 1992. HPC-1 is associated with synaptotagmin and omega-conotoxin receptor. *J. Biol. Chem.* 267:24925–24928.

Yoshikami, D., Z. Bagaboldo, and B. M. Olivera. 1989. The inhibitory effects of omega-conotoxins on Ca channels and synapses. *Ann. NY Acad. Sci.* 560:230–248.

Zucker, R. S., and A. L. Fogelson. 1986. Relationship between transmitter release and presynaptic calcium influx when calcium enters through discrete channels. *Proc. Natl. Acad. Sci. USA.* 83:3032–3036.